Hypersensitive intercellular responses of endometrial stromal cells drive invasion in Endometriosis

Chen-Wei Chen [#, 1], Jeffery Chavez [#, 1], Ritikaa Kumar [1], Virginia Arlene Go [2], Ahvani Pant[1], Anushka Jain[1], Srikanth Polusani[1], Matthew J. Hart[4], Randal D. Robinson[2], Maria Gaczynska[3], Pawel Osmulski[3], Nameer B. Kirma[3], Bruce J. Nicholson[1*]

[1]Department of Biochemistry and Structural Biology, UT Health San Antonio, Texas, USA
[2] Department of Obstetrics and Gynecology, UT Health San Antonio, Texas, USA
[3] Department of Molecular Medicine, UT Health San Antonio, Texas, USA
[4] Center for Innovative Drug Discovery, UT Health San Antonio, Texas, USA

Abbreviated Title: Gap junctions and Endometriosis invasion

[#] Equal contributions as first authors

*Corresponding author
nicholsonb@uthscsa.edu (BJN)

Abstract

Endometriosis is a debilitating disease affecting 190 million women worldwide and the greatest single contributor to infertility. The most broadly accepted etiology is that uterine endometrial cells retrogradely enter the peritoneum during menses, implant and form invasive lesions in a process analogous to cancer metastasis. However, over 90% of women suffer retrograde menstruation, but only 10% develop endometriosis, and debate continues as to whether the underlying defect is endometrial or peritoneal. Processes implicated in invasion include: enhanced motility; adhesion to, and formation of gap junctions with, the target tissue. Endometrial stromal (ESCs) from 22 endometriosis patients at different disease stages show much greater invasiveness across mesothelial (or endothelial) monolayers than ESCs from 22 control subjects, which is further enhanced by the presence of EECs. This is due to enhanced responsiveness of endometriosis ESCs to the mesothelium, which induces migration and gap junction coupling. ESC-PMC gap junction coupling is shown to be required for invasion, while coupling between PMCs enhances mesothelial barrier breakdown.

INTRODUCTION

Endometriosis is a chronic inflammatory disease affecting ~10% of reproductive age women, or 190 million worldwide [Shafrir et al., 2018], characterized by the presence of endometrial tissue in extrauterine lesions on the pelvic peritoneum, ovary and bowel surface. In the US, endometriosis is diagnosed in 35-50% of women with pelvic pain, and up to 50% of women with unexplained infertility (Rogers et al., 2009). Reliable diagnosis requires invasive abdominal surgery, resulting in an average delay of 6.7 years from symptom onset to diagnosis, with 2/3rds of patients being mis-diagnosed at some point [Bontempo and Mikesell, 2020]. Thus, the disease imposes a significant socioeconomic burden of ~$80 billion per year for the US alone between prolonged healthcare costs, and loss of productivity [Soliman et al., 2016]. Treatment of the disease is also limited to excision of lesions, which usually return, or hormonal management of pain, which only further compromises fertility.

The most widely accepted model for the pathogenesis of endometriosis is retrograde menstruation, in which sloughed endometrial tissue during menses traverses the fallopian tubes (or perhaps in rare cases enters the lymphatic or blood circulation) and when deposited in the peritoneal cavity, forms invasive lesions that remain sensitive to hormonal cycles [Sampson, 1927]. Other origins of ectopic endometrial lesions, including Mullerian remnants, metaplasia of coelomic stem cells, or endometrial stem cells have also been proposed [Lauchlan, 1972; Mismer et al., 2004; Sasson and Taylor, 2008], which can explain endometriosis in the absence of menstruation, clonal similarities in ectopic lesions and rare male endometriosis. However, the preponderance of evidence indicates that lesions are of endometrial origin (reviewed in Burney and Giudice, 2012). A major outstanding question is why retrograde menstruation, which is estimated to occur in up to 90% of women, would only result in endometriosis in 10% of women [Burney and Giudice, 2012]. One explanation is that there are specific factors that predispose patients to disease development, but it remains unresolved as to whether these lie in the uterus (the “seed”) or the peritoneum (the “soil”). Several studies have reported molecular differences in the eutopic endometrium of women with endometriosis [Burney et al., 2007; Rogers et. al., 2009; Ulukus et. al., 2006; Yu et al.,2014; Lin et al., 2021], including enhanced survival [Jones et al., 1998] and invasive potential [Lucidi et al., 2005] that could promote lesion formation in the pelvic cavity [Guo et al., 2004; Hastings and Fazleabas, 2006, Tamaresis et al., 2014]. But changes in peritoneal factors can also contribute, including hormonal environment [Parente Barbosa et al., 2011], oxidative stress, inflammation [Augoulea et al., 2012], and decreased immune clearance [Oosterlynck et al., 1991]. The problem remains to distinguish which of these changes are consequences as opposed to causes of the disease, an issue that requires a greater understanding of invasive mechanisms.

While much work has been done on the consequences of endometriosis in terms of inflammation, hormone responsiveness and impact on fertility, little has focused on the initial causes of lesion formation. We know from other invasive processes like metastasis, that such behavior requires enhanced migratory behavior, typically after an epithelial to mesenchymal transition, followed by contact mediated intercellular interactions between the invading and target tissues. These involve initial adhesion and subsequent gap junction formation that has been proposed to trigger disruption of the barrier functions of the target tissue, although understanding of specific mechanism are still limited. Gap junctions, composed of connexin (Cx) proteins encoded by a family of 21 GJ(A-D) genes, mediate direct contact and communication between most cells of the body via exchange of ions as well as metabolites

and signaling molecules <1kD [Goldberg et al, 1999; Weber et al., 2004; Hernandez et al. 2007].

Gap Junctions have been implicated in other invasive processes, like metastasis. In a global screen of cervical squamous carcinoma, Cx43 emerged as one of three genes (along with PDGFRA2 and CAV-1) central to cancer invasion and metastasis [Cheng et al., 2015]. Interestingly, expression of functional gap junctions is suppressed in most primary tumors, as they suppress growth, But significant induction of Cx43 and/or Cx26 gap junctions, either by increased expression or trafficking to the cell surface [Kanczuga-Koda et al., 2006], has also been associated with metastatic breast cancer [Naoi et al. 2007; Stoletov et al., 2013], prostate cancer (Zhang et al., 2014; Lamiche et al., 2012), and melanoma (Ito et al., 2000). GJs appear to exert their effects both during intravasation and extravasation [el Sabban and Pauli, 1991, 1994; Ito et al., 2000, Naoi et al, 2007], as well as forming hetero-cellular GJIC with the target tissue that pass miRNAs or cGAMP to promote target receptivity and an inflammatory environment [Lamiche et al., 2012; Hong et al., 2015; Chen et al., 2016].

Gap junctions have also been associated with multiple aspects of the other major pathology of endometriosis, infertility, GJs have also been shown to be involved from the earliest phases of oocyte meiosis [Simon et al, 1997; Richard and Baltz, 2014] to endometrial= decidualization [Kaushik et al., 2020], blastocyst implantation [Grummer et al.,1996: Diao et al., 2013], and vascularization of the endometrium during pregnancy [Laws et al., 2008].

Despite these links between GJs and the two major pathologies of endometriosis, studies have been limited to tracking connexin expression. Immunocytochemistry showed a shift in Cx expression of endometrial epithelial cells (EECs) from primarily Cx26 *(GJB2)* with some Cx32 (*GJB1*) in the uterus, to Cx43 *(GJA1)* in peritoneal (ectopic) endometriotic lesions (Regidor et al., 1997). A similar switch in EEC Cx expression profile was reported eutopically in the uteri of baboons with endometriosis [Winterhager et al., 2009], but this was not seen in human patient samples where Cx expression of EECs remained unaltered [Yu et al., 2014]. In contrast, endometrial stromal cells (ESCs) have been reported to retain Cx43 expression in both eutopic and ectopic locations, although at significantly reduced levels in endometriosis patients [Nair et al., 2007, Yu et al, 2014]. The reduced Cx43 expression in the uterus has been suggested to contribute to infertility associated with endometriosis [Yu et al, 2014], but to date no studies have explored the role of GJs in lesion formation. Of particular relevance to this is the consistent observations, mentioned above, that connexin expression is repressed in primary tumors, yet is induced in metastatic tumor cells to promote invasion. We investigate this same connection here with regard to endometriosis using primary endometrial stromal and epithelial cells isolated from 22 control and 22 endometriosis patients from stages I-II and III-IV of the disease **(Table 1)**.

RESULTS

ESC and EEC mixes from endometriosis patients are more invasive, with ESCs being the primary invaders.

As the first step in lesion formation, or any invasive process, is adhesion to the target, we tested the two major endometrial cell types for adhesiveness to mesothelial cells, as this would indicate which cell type we should focus on as the primary instigator of invasion. Peritoneal Mesothelial Cells (PMCs, specifically the LP9 cell line) or primary EECs or ESCs isolated from patients as described in Methods (see **Fig. 1 - figure supplement 1**) were attached to the cantilever of an Atomic Force Microscope (AFM) and brought into contact with

LP9 mesothelial cells in a monolayer, and after 30 seconds, the force needed to separate the cells was measured [**Fig. 1A** - Sancho et al., 2017; Roca-Cusachs et al., 2017)]. PMCs show low levels of adhesion to one another and to EECs, but 6-fold greater forces were needed to separate ESCs from PMCs **(Fig. 1B)**. These measurements were conducted with cells from control patients. ESCs from endometriosis patients showed even higher levels of adhesion, as they were difficult to separate from PMCs even after only 1-2 seconds of contact, precluding accurate measurement of force using our instrumentation.

We then directly assessed invasiveness using an established 3D-invasion model [Nair et al 2008]. Endometrial cells labelled with a lipophilic fluorescent dye (Di-O) are dropped onto a hormone depleted Matrigel coated Boyden chamber on which is grown a confluent monolayer of the LP9 PMCs **(Fig. 1C)**. Neither ESCs nor EECs invaded through the membrane alone, confirming a dependence on a PMC monolayer for invasion. PMCs alone showed limited invasiveness, but this was excluded as only Di-O labeled cells were counted. Comparisons of ESC and EEC invasiveness from all patients showed ESCs to be 2-fold more invasive **(Fig. 1D)**, consistent with their higher level of adhesiveness to PMCs observed above. This led us to focus our invasion comparisons between control (8) and endometriosis (11) patients primarily on ESCs. ESCs from endometriosis patients were 4-6 fold more invasive than from controls **(Fig. 1E)** mostly due to patients from more advanced disease **(Fig. 1 - support data 1)**. This difference was less (~2.5 fold) when invasion was measured in the absence of a serum gradient, or at higher gradients (data not shown), indicating that endometriosis ESCs are more responsive to low-level chemo-attractant gradients. We also observed a similar difference of ~4 fold when we compared invasiveness across PMCs derived from either control or endometriosis patients (**Fig. 1E)**.

In the retrograde model of endometriosis, fragments of endometrium, containing both ESCs and EECs, invade the mesothelium, explaining why both cell types are found in endometriotic lesions. So while EECs alone were less invasive, we did test the effect of mixed ESC/EEC cultures in invasion across PMCs, but in the absence of an attractive serum gradient to more closely mimic *in vivo* conditions. When EECs were mixed in equal numbers with ESCs they enhanced invasion by 1.5-fold in control samples (n=9), and 2.1-fold in endometriosis samples (n=8), but this was only significant ($P<0.01$) in endometriosis samples **(Fig. 1F)**. Differential labeling the two cell types (**Fig. 1 - Figure supplement 2)** confirmed that ESCs were the primary invading cells, with EECs making up 20% and 40% of the invading cells in controls and endometriosis, respectively **(Fig. 1 - source data 1)**.

While most endometriosis lesions are restricted to the peritoneal cavity, some (<5%) can be found outside, even as far as the lungs and brain. Such lesions clearly cannot arise form retrograde menstruation, but as we have shown that ESCs from patients are highly invasive through PMCs, we tested whether they may also be able to intravasate into the circulation, allowing further spread. A comparison of 8 patients with different invasive tendencies demonstrated that invasiveness across a PMC monolayer was highly correlated with invasiveness across an endothelial cell monolayer of HUVECs **(Fig. 1G)**, suggesting that spread on endometrial cells through the circulation may also be enhanced in endometriosis.

ESCs from endometriosis patients show greater inherent motility, and this is further enhanced by PMCs.

To assess another major contributor to invasiveness, we compared motility of ESCs from control and endometriosis patients using a wound healing assay **(Fig. 2A** and **B).** Comparisons of ESCs from 15 control and 11 endometriosis patients (4 stage I-II and 7 stage

III-IV) revealed a 2-fold increase in motility associated with disease **(Fig. 2C)**. In a subset of these patient samples (8 controls and 4 endometriosis patients) we also tested the effects of co-culture of ESCs with LP9 PMCs. The motility of co-cultures compared to ESCs grown alone was not significantly changed in control samples but increased by 1.5-fold in endometriosis samples **(Fig. 2D).** We could not assess the effect of EECs on ESC motility due to low adhesiveness of EECs, leading to selective loss of these cells and disruption of the cell monolayer needed for motility measurements. While these data show a net 3-fold difference in motility between control and endometriosis ESCs in the presence of PMCs, this does not fully account for the 6-fold difference in invasiveness, indicating that additional factors play a role.

Peritoneal mesothelial cells (PMCs) induce Gap Junction Intercellular Coupling (GJIC) with ESCs.

Adhesion, motility, and invasive processes have all been shown to be regulated at some level by gap junctions, either between like cells or between invading cells and the target tissue. To explore the potential role of GJs in endometriosis, we utilized an automated variant of the "parachute" technique to measure GJIC as the rate of spread of preloaded calcein dye from donor cells (D) dropped onto a monolayer of acceptor cells (A) (**Fig. 3A**). While we had observed some changes in the expression of gap junction genes in ESCs and EECs with endometriosis [Chen et al., 2021], we saw only modest changes (<35%) in the most highly expressed isoform, Cx43 or in homo-cellular GJIC between ESCs (**Fig. 3B**) between control (black) and endometriosis (grey) patients. However, hetero-cellular GJIC between ESCs and PMCs, as would occur at the onset of lesion formation, was induced at higher levels as disease progressed **(Fig. 3C)**, from 2-fold in controls to over 3-fold in stage III-IV endometriosis ($P<0.01$).

Since the induction of GJIC was observed within the 2 hour timespan of our coupling assay, it seemed likely it was not due to transcriptional activation. Thus, we examined the distribution of Cx43 protein in ESCs before and after contact with PMCs **(Fig. 3D-K).** ESC cultures alone show most of the Cx43 staining is intracellular, particularly evident in non-confocal images **(Fig. 3D-E).** Some punctate staining at cell-cell interfaces indicative of gap junction plaques (arrowheads) is evident, particularly in confocal images (**Fig. 3F-G**). By contrast, in mixed ESC/PMC cultures there is much reduced intracellular staining within most, although not all, ESCs (green * labelled cells in **Fig. 3 H, I and K**). Punctate staining at cell-cell interfaces is now more frequently observed between ESCs and PMCs (solid yellow arrowheads), as well as between ESCs (green filled yellow arrowheads) (**Fig. 3 H** and **J**). These gap junction plaques are often found on PMC processes that cross ESC cell bodies **(Fig. 3K**), or the reverse, and are far more frequent in ESC-PMC co-cultures than in ESC homocellular cultures.

GJIC is required for invasion of ESCs across a peritoneal mesothelium.

As GJIC has been indirectly linked to the analogous process of extravasation (Ito et al, 2000: Naoi et al., 2007), we directly tested if GJIC between ESC and PMCs is required for invasion across the mesothelium. We employed several complementary strategies to selectively block GJIC, targeting Cx43, as it is expressed at 10 times higher levels than other connexins in both control and endometriosis ESCs as well as PMCs [Chen et al., 2021].

Firstly, we pre-treated both PMCs and ESCs in our invasion chambers with GAP27, a peptidomimetic of part of the second extracellular domain of Cx43 that has been shown to

block the formation of gap junctions between newly contacting cells [Evans and Leybaert, 2007]. GJIC was blocked ~85% in both control (black) and endometriosis (grey) derived ESCs. This resulted in a reduction of invasiveness of ESCs through the PMC monolayer, although this was only significant (70%) in cells derived from endometriosis patients (**Fig. 4A**, n=6). In subsequent experiments, we found the effectiveness of GAP27 to block GJs and invasion to be variable, presumably due to variability between vendors and batches of the peptide. So we moved to Cx43 KD approaches.

Our first approach was to use transient transfection of siRNAs to Cx43. While these did achieve 60-70% KD of GJIC, and significant (~40%) block of invasion, results were highly variable due to compromised cell health following transfection. This affected both the effective formation of a mesothelial barrier by as PMCs, and the motility and invasiveness of ESCs. Thus, to avoid these complicating effects of transient transfection, we moved to stable Lentiviral infection to generate PMCs and ESCs that express inducible shRNAs targeted to Cx43 (or scrambled shRNAs as control). An RFP reporter allowed us to track which cells expressed the shRNA, which averaged 61 ± 8% (n=8) of the cell population in the presence of doxycycline. Suppression of Cx43 protein levels in the total cell population was evident **(Fig. 4B**) and GJIC was inhibited by 95 ± 4% (n=7) in infected ESCs (**Fig. 4C)**. Invasion by infected ESCs expressing Cx43 shRNA (identified by RFP expression) was reduced by 90-95% compared to uninfected cells in the same sample (**Fig. 4D**). In the inverse experiment where Cx43shRNA was expressed in PMCs, the monolayer consisted of both infected (~70%) and uninfected cells, but invasion was still inhibited by ~85% **(Fig. 4D)**.

Finally, to ensure the inhibition of invasiveness was due to block of GJIC, and not loss of the adhesive roles of gap junctions (since we had reduced total Cx43 levels), we used the same Lentivirus system to express a dominant negative Cx43 construct, Cx43T154A (DN Cx43) in either ESCs or PMCs, with ~70% efficiency. This DN construct forms structurally normal gap junctional plaques but prevents channel opening when co-expressed wtCx43 [Beahm et al, 2006]. Expression of DN Cx43 increased total Cx43 levels by ~2 fold in ESCs and 1.4-fold in PMCs **(Fig. 4B)**. Invasive behavior of infected ESCs (identified by GFP reporter expression) was reduced by >98% compared to uninfected cells in the same sample **(Fig. 4D).** Expression of the DN isoform in PMCs produced a mixed monolayer of infected (~70%) and uninfected cells and resulted in a 65% block of invasion.

While each method for blocking gap junctions may have limitations, we demonstrate that four independent approaches that block either functional GJIC between ESCs and PMCs (GAP27 or DN CX43) or expression of Cx43 in either of the cell types (si- and shRNA) all significantly reduce invasive behavior of ESCs. The fact that block in both ESCs and PMCs caused similar effects strongly implicates a role for gap junctions between these two cell types, as if hemichannels are involved, they would have to have similar effects in both cell types.

Cx43 expression is required for both the integrity of a mesothelial barrier and its disruption by ESCs.

To probe the influence of ESCs, in the presence or absence of Cx43, on the “barrier function” of the mesothelium (ie. the intercellular contacts between PMCs comprised of tight and adhesive junctions that prevents transmigration of cells), we utilized the unique ability of AFM to probe the surface topology of a cell monolayer in real time. ESCs from control subjects or endometriosis patients were first labeled with the membrane dye DiO, and dropped onto a PMC monolayer at a ratio of ~1:20 (ESC:PMC). After ~3 hrs, the monolayer was imaged with AFM using a ‘sharp’ conical probe at a constant applied pressure of 1 nN to obtain a 3-D

contour map of the monolayer **(Fig. 5B)**. This readily identified the interfaces between cells and measured the depth of penetration of the probe between cells as a physical measure of mesothelial "barrier function" **(Fig. 5A)**. ESCs from several patients all induced a widening in the gap between PMCs **(Fig. 5C)**, corresponding to an ~2-fold increase in penetrance, measured ~10µm (1-2 cell diameters) from an identified dropped cell. This increase in penetration of the monolayer was seen with all ESCs but was which was more notable in ESCs from endometriosis patients (**Fig. 5D**), consistent with their greater invasive potential **(Fig. 1E)**.

We then used Cx43 shRNA, DNCx43 and wtCx43 infected LP9-PMCs, characterized in **Fig 4 B-D,** to test the dependence of these changes on GJIC. First, we observed that the "barrier function" of a PMC monolayer in the absence of ESCs was dependent on Cx43 expression, as the degree of penetrance was reduced when Cx43 was overexpressed and increased when Cx43 was inhibited by shRNA **(Fig. 5E)**. This is consistent with GJs being part of the intercellular nexus, including tight and adhesions junctions, that connect cells. However, this effect was strikingly inverted when we introduced ESCs **(Fig. 5F)**. Cx43 overexpression in PMCs significantly enhanced penetrance in response to ESCs, while Cx43 inhibition by shRNA eliminated the effect of ESCs, so that penetrance was indistinguishable from control PMC monolayers. The only difference between the studies in **Figs. 5E and F** is the presence of ESCs in the latter, implicating the formation of GJs between ESCs and PMCs as the factor that must trigger the breakdown of the PMC barrier. This directly demonstrated that this was dependent on Cx43 channels, as expression of a DN Cx43 in PMCs, which suppresses coupling but maintains the gap junction structures, and all their adhesive and structural properties, also prevented barrier breakdown similarly to Cx43 shRNA.

This raised the question that if GJs pass signals from ESCs to PMCs that promote breakdown of the mesothelial barrier, do gap junctions between PMCs also play a role in propagating such a signal distribution through the mesothelium. To test this, we dropped ESCs at a lower density (1:50 ratio with PMCs) and measured the degree of penetrance between PMCs at increasing distances from a single contacting ESC **(Fig. 6A)**. ESCs from stage I-II patients, which showed only modest induction of ESC-PMC coupling, were compared with ESCs from stage III-IV patients, which showed much greater levels of ESC-PMC coupling **(Fig. 6B)**. When penetrance was plotted against distance from a dropped ESC, the influence of the ESCs decayed to background levels at much greater rates in the case of poorly coupled ESCs (Endom. stage I-II) than well coupled ones (Endom. stage III-IV), propagating over distances of 200 µm to >700 µm, respectively **(Fig. 6C)**. As expected, knock-down of Cx43 by shRNA in the LP9 cells eliminated all effects of the ESCs. However, overexpression of Cx43 in LP9 PMCs caused a dramatic extension of the propagation range to beyond the limits of our recording at 800µM **(Fig. 6D),** corresponding to over 40 cells from the dropped ESC.

DISCUSSION

Despite afflicting 10% of the female population, the etiology of endometriosis is still the subject of debate. Retrograde menstruation of endometrium into the peritoneal cavity is the most widely accepted theory to explain most endometriosis cases. However, why is endometriosis seen in only 10% of women, when ~90% display retrograde menstruation? Are there specific changes in the uterine endometrium (the "seed") or the peritoneal lining (the "soil") that predispose patients to develop the disease? Most studies have focused on expression changes in endometrial cells in utero, or from established lesions, or on the inflammatory sequalae of the disease. Few studies have examined the initial stages of lesion

formation that could provide mechanistic insights into disease pathophysiology and most directly address the issue of a “seed” or “soil” origin. We have taken a reductionist approach to the problem by isolating and characterizing each major cell type involved in initial lesion formation from control (19) and endometriosis (22) patients: endometrial epithelial (glandular) and stromal (supporting) cells (EECs and ESCs, respectively) from control and endometriosis uterine biopsies, and peritoneal mesothelial cells (PMCs), both established LP9 cells and isolated from control and endometriosis patients (characterized in [Go etal.,2024]).

Of the endometrial cells, the major focus was on ESCs, as they proved more adhesive to PMCs, more motile, and ultimately twice as invasive as EECs from the same patients. ESCs from endometriosis compared to control patients were also more adhesive to PMCs, more motile (~2-fold) and much more invasive across PMCs (2-6 fold depending on disease stage). EECs were mixed with ESCs to mimic in vivo conditions, invasiveness was further enhanced, but this was only significant in endometriosis samples, which also showed a higher fraction of EECs in the invading cell population than controls (40% compared to 15%). Our experiments were conducted on primary cells cultured from pipelle endometrial biopsies, which leaves open the possibility that stem cells present in the endometrium could be included in our sample, although they may differentiate into one of the main cell types in culture.

Our observations that endometriosis derived ESCs show increased responsiveness to other cell types, including enhanced motility and adhesion to, gap junction communication with, and invasion across PMCs, combined with prior findings that endometriosis endometrial cells show enhanced repression of apoptosis [Taniguchi et al., 2011], and immune avoidance [Han et al., 2015; Bjork et al., 2024], strongly implicate changes in the endometrium as causative of the disease. The most direct deduction from these results is that the 10% of patients that develop endometriosis are distinguished from the 80% that have retrograde menstruation without endometriosis by pre-existing changes in the endometrial lining that predispose the cells to an invasive phenotype.

One important question is the extent to which endometrial cell behaviors are affected by the menstrual phase, birth control, or other variables between patients. We compared invasiveness, motility and induction of GJIC by PMCs between control and endometriosis ESC in patients from the proliferative or secretory phases of the menstrual cycle or those on oral contraceptives. While the limited numbers precluded applying robust statistics, under all menstrual conditions the endometriosis cells showed enhanced activity of each phenotype. Among endometriosis patients, where we had 3-6 patients in each group, we also compared each ESC phenotype from patients in different menstrual conditions (cycle stage or oral contraceptives). No statistically significant differences were observed, suggesting modest hormonal influences on the aspects of ESC behavior associated with invasion. Any minor differences are outweighed by the disease phenotype.

Since we could not assess endometrial samples patients prior to disease manifestation, it is certainly possible that some of the changes we observe may be a consequence of the disease through feedback from lesions in the peritoneum that can globally affect hormonal levels and inflammatory responses. Indeed, such effects could explain the observations in Nirgianakis et al. (2020) that a significant number of patients (48%) presenting initially with superficial lesions can show more deep infiltrating lesions on recurrence. Delineating the degree to which endometrial changes pre-exist disease onset will remain a challenge based on both practical and ethical considerations governing human trials. The only thing that is clear from the studies of Go et al. (2024) is that the invasive behavior of ESCs is not influenced by PMC origin (from control or endometriosis patients), only by ESC origin.

While others have compared other aspect of endometrial behavior [Taniguchi et al., 2011; Han et al., 2015; Bjork et al., 2024], we have focused on their invasive behavior and interactions at the mesothelial lining. The enhanced invasiveness of eutopic ESCs from Endometriosis patients across PMCs seems in large part to be due to their enhanced responsiveness to PMC signals that increase GJIC and motility. This result is consistent with our prior CyTOF single cell Mass Spectroscopy comparisons of ESCs alone and in co-culture with PMCs that showed much larger shifts in expression of markers of EMT plasticity (ZEB1, SNAIL1, TWIST) in endometriosis than control derived ESCs [Li-Ling et al, 2021]. That ESCs also increase invasiveness when co-cultured with their cognate EECs, suggests that the hypersensitivity of endometriosis ESCs is not restricted to PMCs.

Many of these changes parallel those observed in metastatic cancer, including the enhanced motility, target induced changes in EMT plasticity [Lambert et al, 2017], and ability to breakdown tissue barriers during intra- and extra-vasation and metastatic invasion. In the latter processes, one of the earliest steps is formation of gap junctions between the tumor cell and endothelium [El Sabban et al., 1991 and 1994; Ito et al., 2000; Naoi et al, 2007] or target tissue [Stoletov et al., 2013; Hong et al., 2015; Chen et al., 2016]. In fact, GJ are typically suppressed in primary tumors, but need to reactivate in order to metastasize [Wu and Wang, 2019], which is often associated with more efficient transport of connexins to the cell surface [Kanczuga-Koda et al., 2006]. We demonstrate here a very analogous process in endometriosis. GJ expression [Yu et al., 2014; Chen et al, 2021] and cell coupling are suppressed eutopically but then GJ coupling is strongly induced ectopically when ESCs encounter PMCs through trafficking of intracellular Cx43 stores to cell-cell interfaces. By further analogy with metastasis, the invasiveness of ESCs across the mesothelium is shown here to be highly correlate with their invasiveness across an endothelium. This is important in terms of disease, as the low incidence of endometriosis outside of the peritoneum has been used to argue that lesions may arise from non-endometrial cells such as stem cells or Mullerian remnants. However, it seems that the same features that make ESCs more invasive in the peritoneum In endometriosis, also increase their chances of entering the bloodstream.

GJ coupling has been associated with enhanced motility in cancer cells [Zhang et al., 2015; Polusani et al., 2016] and may play a role in PMC induction of ESC motility seen here, although this was not directly tested. However, we do clearly demonstrate that this induced GJ coupling between ESCs and PMCs is required for disruption of the mesothelial barrier and invasion, something that has not been definitively established in metastasis. As illustrated in **Fig. 7**, we propose that contact between ESCs and PMCs induces trafficking of Cx43 to the surface and formation of ESC-PMC gap junctions that mediate the transfer of yet to be identified intercellular signals that initiate the disruption of the intercellular junctional nexus that prevents trans-mesothelial migration. The adhesive roles of gap junctions do not appear to play a major role, as the DN Cx43T154A, which preserves junctional structures, but prevents channel opening (Beahm et al, 2006), also inhibits invasion. Release of signals through Cx43 hemichannels also seems unlikely, since invasion can be similarly prevented by KD of Cx43 in either ESCs or PMCs.

It is interesting to note that we demonstrate here that PMC GJs promote mesothelial integrity under normal conditions, possibly through nucleating other junctional structures between cells (e.g. tight and adhesions junctions) with whom they share many accessory and cytoskeletal binding proteins (e.g. ZO1, β-catenin, etc.). But apparently this proves to be an Achilles heel when ESCs arrive in the peritoneum, as now the GJs between PMCs mediate

further propagation of intercellular signals leading to breakdown of mesothelial intercellular contacts at significant distances from the site of ESC contact **(Fig. 7B, lower panel)**.

Together, these studies demonstrate that eutopic ESCs (i.e. from the uterine endometrium) are very distinct in endometriosis and control patients, the former being characterized by enhanced responsiveness to interactions with EECs and PMCs that promote invasive behavior. Gap junctions between ESCs and PMCs, and within the mesothelium, are shown to critical in initiating lesion formation through mutually induced changes in the phenotypes of both cells. Together these results demonstrate that changes within the uterine endometrium prime ESCs to be invasive once they reach the peritoneal cavity. There seem to be many parallels with the development of metastatic potential in cancer cells, which is likely determined before they leave the primary tumor, and also involves an induction of gap junction formation that facilitates invasive behavior. Our data also supports a “seed” (endometrium) rather than “soil” (mesothelium), origin for endometriosis, which is more definitively established in Go et al., 2024.

MATERIALS AND METHODS

Primary endometrial epithelial cell isolation from endometrial biopsies

Primary ESCs and EECs were isolated from endometrial biopsies obtained from women with and without endometriosis under IRB protocol # 20070728HR (8-31-23). All women provided informed consent prior to participating in this Institutional Review Board approved protocol. Study subjects were premenopausal women between 30 and 45 years of age with regular menstrual cycles, or in some cases on Oral Contraceptives, undergoing laparoscopic surgery for gynecologic indications (**Table 1**). Women with pelvic inflammatory disease/hydrosalpinx, endometrial polyps, or submucosal fibroids were excluded. Two control patients (H11 and H20) and one Endometriosis patient (31) were found to have ovarian cysts at the time of surgery. Endometriosis was staged according to the revised American Society for Reproductive Medicine (ASRM) criteria and confirmed by histopathologic review of peritoneal or cyst wall biopsy in all cases. Fertile women undergoing tubal sterilization and without endometriosis at surgery were considered healthy controls. Menstrual cycle phase (proliferative or secretory) was determined by cycle history and confirmed by serum estradiol and progesterone levels when available. Endometrial tissue was obtained by pipelle biopsy at the time of laparoscopic surgery. In some patients, during laparoscopy for definitive diagnosis of disease, small biopsies of the peritoneum were also taken both in the vicinity of, and distant to, identified lesions. These samples were kept on ice for <2hrs before embedding in OCT and freezing and storage at -80^{0}C for subsequent immunocytochemistry.

Pipelle endometrial biopsy material was dissociated by shaking in 5mg/ml collagenase and 2.5mg/ml DNase in Hanks Balanced Salt Solution at 37^{0}C for 1 hour. Isolation of primary ESCs and EECs from the biopsies was performed using a combination of straining (45uM nylon filter) and differential sedimentation (EECs cluster and sediment faster), followed by differential attachment (EECs adhere less well to culture plates), in a modification of the method developed by Kirk and Irwin (1980) used in prior studies [De La Garza, et al., 2012; Chen et al., 2016]. In some experiments the differential attachment step was replaced by using an Ep-CAM affinity column to enrich EECs. Both methods achieve about 97% purity for EECs and ESCs, as illustrated in **Fig. 1 – figure supplement 1** by immunostaining for epithelial [EpCAM- ab71916 from Abcam, Waltham, MA) and CK 7 (ab902 and 1598 from Abcam)] and stromal [Vimentin (MA1-10459 from Thermo Fisher, Waltham, MA; NBP1-92687 from NovusBio, Centenial, CO)] markers

Cell Culture

Primary ESCs were cultured in Dulbecco's Modified Eagle Medium (DMEM)/F12 (1:1) (Gibco, Buffalo, NY) containing antibiotic/antimycotic mix (Gibco, Buffalo, NY), 10 µg/ml insulin (Sigma, St. Louis, MO) and 10% heat inactivated fetal bovine serum (FBS - Gibco, Buffalo, NY) as described previously (Ferreira *et al.*, 2008). EECs were cultured in MCDB/Medium 199/MEMα (1:1:0.6) containing antibiotic/antimycotic mix, 10ug/ml insulin, D-Glucose (0.45%) (Sigma, St. Louis, MO), Gluta-Max and 10% FBS (Gibco). Prolonged culture was in defined KSFM with supplement, 1% FCS and antibiotics/antimycotics (Gibco) to preserve differentiated state of the EECs [Chen et al., 2016] although this generally was only possible to 3 - 4 passages. All experiments were performed using low passages ($\leqslant$4) to avoid loss of differentiated characteristics. Established LP9 cells (Karyotype verified from NIA Aging Cell Culture Repository #AG07086 PDL 4.84 passage 6, Coriell Institute, Camden, NJ) were used as a model for peritoneal mesothelium and cultured as described previously [De La Garza, 2012, Liu *et al.*, 2009)] and grown in MCDB 131.Medium 199 (1:1 - Gibco) with 15% FBS, sodium pyruvate, Gluta-Max, antibiotic/antimycotic mix (Gibco), 20ng/ml hEGF and 0.4ng/ml hydrocortisone (Sigma, St. Louis, MO). All cells used were confirmed to be mycoplasma free. Previous studies, including our work, have validated and used LP9 cells as a model peritoneal mesothelial line for peritoneal invasion by endometrial cells [Nair et al., 2008]. Primary peritoneal mesothelial cells from control or endometriosis patients (from regions not containing lesions) were cultured form explants as described in Go et al (2024). Identity and purity of all cell cultures were confirmed by immunocytochemistry, using antibodies for Vimentin or CD10 for ESCs, CK 7 for EECs (**Fig. 1 – figure supplement 1)** and Calretenin (ab92341- Abcam) for PMCs.

Trans-mesothelial Invasion Assay

The 3-D invasion assay modeling trans-mesothelial invasion **(Fig. 1C)** has been described previously [De La Garza et al., 2012, Ferreira *et al.*, 2008, Nair *et al.*, 2008)]. Briefly, LP9 peritoneal mesothelial cells (PMCs) were grown to confluence in 24-well invasion chamber inserts containing growth-factor-reduced Matrigel^{TM}, coated on 8-µm pore membranes (Corning, NY). ESCs were labeled with the lipophilic dyes DiO (Invitrogen/Thermo-Fisher), trypsinized and counted, prior to dropping onto the confluent layer of LP9 PMCs in the prepared inserts (~20,000 cells per insert). Media above the insert was replaced immediately prior to the assay with serum free stromal media, and below with 1% serum in stromal media, although other serum gradients were tested After 24 hr incubation, non-invading cells on the upper surface of the insert were mechanically removed. Invading cells on the bottom of the membrane insert, were stained with DAPI, and 10 fields counted using an Inverted Nikon 2000 fluorescence microscope with 20x objective, confirming in each case that the DAPI stained nuclei were associated with DiO staining. In ESC/EEC mixed cell studies, the cells were labelled before mixing with DiO and DiI, respectively, and serum-free stromal media was used on top with 1% FBS containing stromal media on the bottom. In the case of mixed stromal and epithelial invasion studies, LP9 mesothelial media was used on top and stromal media used on the bottom (i.e. no attractive serum gradient). Invasion assays for each cell type were performed in triplicate.

Block of Gap Junction Coupling

To test the role of gap junctions in the invasive process, we initially pretreated both the monolayer and dropped cells for 24 hours with 300uM GAP27 (Zealand Pharma, Copenhagen, Denmark) **(Fig. 4A)**. In other experiments (data not shown), Cx43 KD was achieved by a 24 hour pre-treatment of the LP9 monolayer with a combination of two siRNAs to Cx43 (10 pmoles/well or 5nM final concentration) - Ambion™ Silencer™ Select) in OptiMEM (Gibco, NY) with RNAiMAX (1/100 dilution, Invitrogen/Thermo-Fisher), diluted 1:1 with assay media, per manufacturer's instructions. In a final set of experiments **(Fig. 4B-D)**, ESCs, or PMCs were infected with Lentiviruses expressing one of four doxycycline inducible shRNAs directed to Cx43, along with a pIRES RFP to identify the cells expressing the shRNA (TRIPZ vectors – Dharmacon, Lafayette, CO). Lentiviral vectors constructed in house expressing wt or DN Cx43(T154A) with a bicistronic GFP reporter were also used in some experiments.

Western Blotting

To assess effectiveness of viral infections with shRNA to Cx43 or expression of wt or DN versions of Cx43, ~10^7 cells were lysed in 1 ml of standard RIPA buffer, insoluble material spun out at 12,000 rpm for 10 mins prior to assessing protein concentration by a BCA assay kit (#23225-Termo-Fisher). 1.2ug of protein per sample is then solubilized in standard SDS loading buffer with 1mM DTT for 30 mins at RT, then loaded on an automated Western System (Biotechne, Minneapolis, MN) using a 12-230kD Wes separation module cassette according to the manufacturer's instructions. The individual capillary gels within each cassette allow for band fixation, antibody labeling and visualization (using a fluorescent master mix) within the gel. A biotinylated marker set of proteins was run in one lane. Antibodies used were anti-Laminin A/C (#2032-Cell Signaling Technology Danvers, MA) and anti-Cx43 (#3512-Cell Signaling Technology), both at 1/50 dilution.

Immunocytochemistry

ESCs or EECs are plated at ~50K cells per well onto 8 chamber slides (Nunc LabTech II, ….) pre-coated with 100ug/ml poly-D- Lysine for 30 min at 37^0C and grown to 50-90% confluence. In co-culture experiments of ESCs with LP9 PMCs, LP9 cells were plated first and grown overnight to 70-90% confluence before dropping ~20K ESCs pre-labelled with 1/1000 dilution of CellTracker Green (#C2925, Invitrogen/Thermo-Fisher) in serum free media for 30 min at 37^0C. After 4 hours to allow ESCs to attach, cells were either fixed, or in some cases pre-treated and stained with Membrite Fix dye (#30092-T, Biotium, Freemont, CA) at 1/1000 dilution per the manufacturer's instructions to visualize membranes. All cells were washed with PBS with 1mM Ca^{++}/Mg^{++} (CaPBS) prior to fixation with 2% paraformaldehyde (Sigma, St. Louis, MO) for 15 min at RT. Further CaPBS washed preceded permeabilization with 0.25% triton X-100 and 1% glycine in PBS (15 min at RT) and subsequent blocking of non-specific binding with1% Bovine Serum Albumin (BSA) (Sigma, St. Louis, MO) in 0.5% Tween-20 (1 hr at 37^0C or 4^0C overnight). Primary antibody staining was for 3 hrs at RT or overnight at 4^0C in 0.1%BSA, 0.2% Tween-20 in PBS. Primary antibodies used were: anti-Cx43 (#3512 - Cell Signaling Technology) at 1:100 dilution; anti-Cytokeratin 7 for EECs (#902-Abcam) at 1/1000, and anti-Vimentin (#1-92687, NovusBio) at 1/5000 . After CaPBS washes, secondary antibodies to the appropriate species conjugated to Alexa 488 or Alexa 594 (#s 10680 and 11037-Invitrogen) were used at 1:1000 concentration for 1 hr. at room temperature in the dark. After final washes in CaPBS, the chamber grid is removed and a coverslip mounted with slow-fade Diamond mountant with 4',6-diamidino-2-phenylindole (DAPI) (#S36964, Invitrogen) to visualize the nuclei. Cells were imaged on a Nikon 2000 inverted epi-fluorescent microscope.

In some cases superimposed phase images were used to trace the membrane contacts between cells for clarity in visualizing Cx43 localization.

Motility Assays

Motility was assessed by a wound healing assay illustrated in **Fig. 2A-B**. Cultures are grown to confluence in a 96 well plate format before being mechanically wounded and washed. Wound closure is measured every three hours in the Incucyte automated cell monitoring system (Essen Biosciences/Sartorius, MI) over ~3 days. Mixed cultures were plated with 2/3rds primary ESCs with 1/3rd LP9-PMCs. As we found that dye labeling of the cells can affect motility, only bulk migration of the whole culture was measured. % wound closure was platted against time and the linear portion fitted by regression analysis to provide the rates shown. All assays were performed in quadruplicate wells.

Homo-cellular and Hetero-cellular GJIC Assays

GJIC was measured using a novel automated parachute assay. Recipient cells are grown to confluence in a 96 cell flat bottomed plate, and the media changed to (Phenol Red-free DMEM, sodium pyruvate and 5%FBS – Assay Media) immediately before the assay. Donor cells in separate wells are incubated for 20 mins with 10uM calcein AM (Invitrogen/Thermo-Fisher), a membrane permeable dye that on cleavage by intracellular esterases becomes membrane impermeable, but permeable to gap junctions. After washing, trypsinization and addition of assay media, ~2500 calcein-labeled donor cells per well are dropped ('parachuted') onto the recipient cell layer, and calcein transfer between donor and recipient cells observed by fluorescent microscopic imaging (**Fig 3A**). For homo-cellular interactions, ESCs, EECs or LP9 donor cells were parachuted onto recipient cells of the same type. For hetero-cellular GJIC assays, ESCs or EECs were parachuted onto LP9 recipient cells. Fluorescent, bright field and digital phase contrast images of 10-15 fields per well were captured on an Operetta automated microscope (Perkin Elmer) at 30 min intervals for approximately 2 hours. A program (developed in consultation with Perkin Elmer) allowed identification of all cells on the plate, (from phase contrast image), original donors (5-15 per field), and dye-filled recipients (based on calcein intensity). Data are expressed as # of fluorescent recipient cells/# of donor cells for each condition (A/D ratio), plotted over time, and a linear regression line drawn through the data, with the slope used as a measure of coupling and regression coefficient (typically >0.8) used as a measure of assay reliability.

AFM measurements of cell-cell adhesion and mesothelial integrity.

We applied a Nanoscope Catalyst atomic force microscope (AFM, Bruker) interfaced with an epi-fluorescent inverted microscope Eclipse Ti (Nikon, Melville, NY). AFM images were acquired with the Peak Force Quantitative Nanomechanical Mapping (QNM) mode with cells immersed in appropriate culture media. ScanAsyst probes (Bruker, Billerica, MA) with the nominal spring constant 0.4 N/m were used for imaging. The exact spring constant for each probe was determined with the thermal noise method [Butt and Jaschke, 1995]. For each cell culture dish at least 5 fields 100 by 100 μm were collected with the Peak Force set point of 2nN, and electronic resolution of 256 by 256 pixels. Nanomechanical data were processed with Nanoscope Analysis software v.1.7 (Bruker) using retrace images.

Cell to cell adhesion: We attached a tester cell to a cantilever of a tipless probe MLCT-O10 (Bruker, cantilever A, spring constant 0.07N/m) using polyethyleneimine (PEI) as a glue

[Friedrichs et. al., 2013)] **(Fig. 1A)**. Briefly, the probes were immersed in 0.01% PEI in water for 30 min. Tester cells attachment to a culture dish was weakened by replacement of the culture medium with a non-enzymatic cell dissociation solution (Millipore) for 15-30 min in a cell culture incubator (37°C, 5%CO). Next, a single tester cell loosely attached to a culture dish was attached to a PEI covered cantilever by pressing it at 1nN for 5-10 min. After visual inspection of successful cell attachment, the tester cell was lifted and transferred to a dish containing single tested cells. Then the tester cell was positioned over a tested cell and the cantilever slowly lowered till cell-cell interactions were detected with a force plot. The cells were left interacting for 30 to 180 sec at forces 0.5 to 5 nN and then the tester cell was lifted. During this step a force plot was recorded, and the collected data applied to calculate cell – cell adhesion parameters. The force plots were baseline corrected and a maximum of adhesion between cells during their detachment was calculated (units of force, Newton) [Taubenberger, Hutmacher, and Muller 2014; Dufrêne et al. 2017)].

Integrity of LP9 mesothelial monolayer: LP9 cells were grown to confluence in a 60mm culture dish**.** ESC cells grown in separate wells were stained with DiO, suspended, and dropped on to the LP9 monolayer at either a 1:50 or 1:20 ratio to the LP9 cells. In cases where cell mixes were used, ESCs and EECs were labelled with different dyes (DiI and DiO, respectively) prior to mixing in equal numbers and dropping onto PMCs. Three hours later the cells were imaged by AFM **(Fig. 5B-C)**. To calculate a tip penetration depth, cell boundaries were identified using images collected by the peak force error (PFE) channel. To exclude gap areas between cells or areas of cells growing in multilayers, PFE images were overlaid with height channel images after processing them with the flatten function of 1^{st} order. Tip penetration was calculated based on a height histogram of all data points using a difference between the prevalent maximum of cell monolayer height and the prevalent maximum depth between cells accessible for the tip **(Fig. 5A)**.

Data and Statistical Analysis

As data was distributed normally, comparisons of GJIC and invasion of ESC and EEC populations utilized two tailed student t-tests, with a cut-off off of $p<0.05$ (degrees of freedom ranged from 8 – 22). Statistical tests of all AFM data were performed, and corresponding graphs prepared with OriginPro 2020 (Origin Lab).

ACKNOWLEDGEMENTS:

We would like to express gratitude to: the CPRIT funded High Throughput Screening Facility who helped with the assessment of GJIC; the CPRIT-funded Bioanalytics and Single-Cell Core (BASiC) facility at the University of Texas Health San Antonio for AFM analyses; the clinical teams who helped in collection of patient samples, particularly Jessica Perry at UTHealth SA, Peter Binkley, curator of the UTHealth SA Ob/Gyn tissue bank, Dr. Robert S. Schenken who collected initial samples used in our GAP27 studies and Janan van Osdell and Somer Baburek from Hear Biotech Inc who provided patient samples for motility studies; We would also like to thank Taryn Olivas and Taylor Williams who made critical contributions to the early characterization of patient samples and Dr. Li-Ling Lin for her insightful observations on CyTOF studies that helped us interpret our functional findings.

FUNDING:

This work was initially supported by an NICHD award RO1HD109027 to BJN, the Endometriosis Foundation of America (NBK), and generous earlier internal support from UT Health San Antonio through the LSOM Women's Health Initiative (BJN and NBK), a Presidential Entrepreneurial Fund Award (NBK) and a pilot award from the Circle of Hope through the Mays Cancer Center (BJN). GJIC measurements were performed in the High Throughput Facility within the CIDD, funded by CPRIT, (# RP160844) and the Institute for Integration of Medicine and Science (NIH-NCATS grant #UL1 TR 002645). AFM measurements were performed in the BASiC facility at the University of Texas Health San Antonio, which receives funding from CPRIT grant # RP150600.

Table 1: Patient Data

Patient	Etnicity	Age	BMI	Cycle stage
CONTROL				
1	Cauc	22	18.1	OCP
9	NS	35	27	LS
10	Cauc	36	31	irregular
12	Hisp	38	30	unknown
14	Hisp	40	29.2	post-delivery
17	Cauc	23	32.6	ES
21	Hisp	25	28.3	P
25	Afr Am	33	25	ES
30	Afr Am/Hisp	37	43.4	LS
33 *	Hisp	31	39.6	P
34	Cauc	30	38.2	OCP
36	Cauc	36	33.1	M
37 *	Cauc	28	37.3	post-delivery
38 *	Hisp	25	27.7	unknown
45 *	Cauc	33	38	OCP
47 *	Hisp	29	24.5	OCP
H11	Hisp	38	34	P
H19	Cauc	25	28	LS
H20	Cauc	45	25	P
H25	Hisp	26	29	P
H27	Cauc	26	19	P
H47	Cauc	24	33	P
ENDOMETRIOSIS I-II				
4	Hisp	35	22.5	P
16	Pac Isl	30	28	ES
23	Cauc	25	27.4	M
24	Cauc	35	27.6	ES
26	Cauc	24	23.1	MS
27	Cauc	31	31.3	P
31	Hisp	30	25.8	OCP
32	Cauc	39	29.9	P
35 *	Cuac	28	21.7	P
39 *	Hisp/Pac Isl	25	24.2	MS
43	Cauc	25	40.2	MS
ENDOMETRIOSIS III-IV				
2	Cauc	26		M
3	Cauc	31		OCP
5	Afr Am	28	18.9	OCP
6	Cauc	41	45.1	LS
7	Hisp	40	20.3	OCP
13	Cauc	37	23	MS
15	Cauc	23	25	LS
19	Cauc	30	22	P
40 *	Hisp	34	18.9	IUD
41	Cauc	32	23	M
42	Cauc	34	21	OCP

CYCLE STAGE Legend	
OCP	Oral contraceptives
IUD	Intra-uterine device
P	Proliferative
ES	Early secretory
MS	Mid-secretory
LS	Late Secretory
M	Menstruation

*	PMCs also obtained

FIGURE LEGENDS:

Figure 1: Characterization of endometrial cells from control and endometriosis patients.
Adhesiveness: (A) The force needed to separate a cell attached to an AFM cantilever tip (left) from PMCs growing on a dish (left) was calculated from a force/distance curve (right). **(B)** LP9 PMCs show similar adhesion to one another as to EECs, but much stronger adhesion to ESCs (3-6 technical replicates).
Invasiveness: **(C)** A 3-D ex-vivo model measured endometrial cell invasion across a PMC monolayer in a Boyden chamber. **D)** Consistent with their lower adhesion, EECs were 2-fold less invasive than ESCs across all patients. **(E)** ESCs from Endometriosis patients (n=7) were more invasive than those from controls (n=6), both through an LP9 PMCs (>5-fold difference) or primary PMCs (4 fold difference) derived from both control (n=5) or endometriosis (n=3) patients. **(F)** Mixes (1:1) of ESCs and EECs from the same control (n=6) or endometriosis (n=7) patients were 1.5 and 2.1-fold more invasive, respectively than ESCs alone (significance values represent difference of co-cultures from ESCs alone). **(G)** Invasion of ESCs from 8 patients across LP9 PMC or HUVEC monolayers were highly correlated. Number of repeats for each condition in D - F are shown. Significance based on two-tailed T-test. Full data in **Figure 1 - source data 1**. Legend applies to Figures 1-4

Figure 2. Comparisons of motility of patient ESCs.
(A) Motility was measured by rates of wound clousrein in an incucyte system (images at 0, 24 and 48 hours after scraping). **(B)** Motility is measured by fits to the linear portion of the wound closure over time. **(C)** ESCs from endometriosis patients (n=10) show higher motility than from control patients (n=9). **(D)** Mixing LP9 PMCs with ESCs further increases motility of Endometriosis ESCs, while little effect is seen in control ESCs. Number of repeats for each condition are shown. Significance based on two-tailed T-tests. Full data in **Figure 2 - source data 1**.

Figure 3: Coupling between ESCs and PMCs is induced in endometriosis.
(A) Gap junction intercellular coupling (GJIC) was measured by a modified “parachute assay” where calcein loaded donors are dropped onto a monolayer of acceptors of either the same (homocellular) or different (heterocellular) cell type, and calcein transfer is measured as a linear increase in fluorescent acceptor/donor ratio over time. Scale bars are 50μM). **(B)** GJIC between eutopic ESCs decreased progressively with disease, reaching significance in Endometriosis III-IV patients. **(C)** Heterocellular ESC-PMC GJIC was induced compared to ESC homocellular coupling and this increased with disease progression to 2 - 4.5-fold in Endometriosis III-IV patients. **(D–K)** Immunocytochemical staining of Cx43 (red), with cell outlines from phase (yellow) or membrite labeling (blue) superimposed in the lower panels. ESCs alone showed some labelling between cells (arrowheads), but most Cx43 was in intracellular pools **(D-G)**. By contrast, in mixed cultures of PMCs with ESCs [labelled with cell tracker green (*)] there is less intracellular Cx43 labelling and punctate staining of GJs between cells is increased in frequency [Arrowheads: ESC-ESC (green in yellow); PMC-PMC (hollow yellow); ESC-PMC (solid yellow)] **(H-K)**. Nuclei are stained with DAPI. Scale bars are 10 μm. Number of repeats for each condition are shown in B and C, with 8-10 patients in each group. Significance based on two-tailed T-tests. Full data in **Figure 3 - source data 1**.

Figure 4: Invasiveness of ESCs is dependent on Cx43 GJIC.
(**A) GAP27 peptide:** Averaging ESCs from control (black bars, n=3) and endometriosis patients (grey bars, n=6), invasion was inhibited by a peptide inhibitor of GJ channels, GAP27 (percent GJIC compared to untreated shown below each bar).
(B - D) shRNA: (B) Infection of doxycycline inducible Cx43 shRNA into endometriosis ESCs or LP9 PMCs reduced levels of Cx43 protein (arrow) compared to Laminin controls (doublet at ~66kD), while expression of DN or wt Cx43 increased Cx43 expression levels. (% of untreated shown below gel)(see **Fig. 4 – source data 1 and 2**). **(C)** Cx43 shRNA inhibited GJIC by >90% compared to scrambled shRNA in infected LP9 PMCs (black bars, n=3) and Endometriosis ESCs (Grey bars, n=4). **(D)** Invasiveness was inhibited by ~85% in Cx43 shRNA infected compared to uninfected neighbors, whether expressed in ESCs (n=7), or PMCs (n=2)**.** DN Cx43 inhibited invasiveness by 98% when expressed in ESCs, and 65% when expressed in PMCs, where ~70% of the monolayer was infected. N represent independent tests with different shRNAs, with 10 technical replicates of each. Significance based on two-tailed t-tests. Full data in **Figure 4 - source data 3.**

Figure 5: ESCs induce GJ-dependent disruption of the barrier function of a PMC monolayer.
(A) Probing the topological surface of a PMC monolayer using an AFM probe under constant force allows identification of sites of intercellular contact (where penetration of the probe is maximal). **(B-C)** 3-D reconstructions of the surface of an LP9 PMC monolayer alone **(B)** or in the presence of ESCs which induce opening of wide gaps **(C)** (Scale Bars in μm). **(D)** Penetration depth between PMCs increased more with ESCs from endometriosis than control patients. **(E)** PMC monolayer integrity (i.e. lower penetrance) is reduced by Cx43 shRNA KD and enhanced by Cx43 overexpression. **(F)** In contrast, when ESCs are dropped onto a PMC monolayer, the increased penetrance that is induced is eliminated by expression of Cx43shRNA or DNCx43 in the PMCs and is enhanced by Cx43 overexpression. Each dot in D-F represents a single image analysis. Significance based on two-tailed t-test. Full data in **Figure 5 – source data 1-3**.

Figure 6: Disruption of the mesothelial barrier by ESCs is propagated through mesothelial gap junctions.
(A) Using a constant force of 1 nN, the AFM tip was moved over the PMC monolayer progressively further away from a dropped DiI labelled ESC.. **(B)** ESCs from an endometriosis III-IV patient showed greater homocellular (solid grey) and induced heterocellular GJIC with PMCs (striped grey) than those from a endometriosis I-II patient. GJIC of LP9 PMCs was also measured and shown to be decreased by 60% through expression of Cx43shRNA (black). **C)** Penetration through the LP9 PMC monolayer decayed with distance from the dropped ESC much faster in the poorly coupled Endo I-II ESCs (grey) than the better coupled Endo III-IV ESCs (black). Penetration of the monolayer was eliminated by KD of Cx43 in PMCs (red). **(D)** Conversely, the decay in penetration of the PMC monolayer induced by Endo III-IV ESC cells (black) was greatly reduced by over-expression of Cx43 in PMCs (green). Full data in **Figure 6 – source data 1**.

Figure 7: Model of GJIC induction of trans-mesothelial invasion.
(A) In healthy patients, when endometrial cells (light brown) encounter a mesothelium (brick red) following arrival in the peritoneum via retrograde menstruation, there is limited GJIC between ESCs and PMCs. ESCs also likely undergo apoptosis. **(B)** In endometriosis, interactions with mesothelial cells triggers Cx43 trafficking to the cell surface and a significant

enhancement of GJIC. The increased GJIC mediates transfer of signals to PMCs (green triangles), which propagate through the mesothelium, inducing disruption of the adhesive and tight junctions between PMCs, facilitating invasion of the ESCs. There would also be passage of signals from PMCs to ESCs (purple dots) that induce further changes in ESCs that could promote invasion (Ling et al, 2021). EECs (green cells) show minimal invasion alone, but can enhance ESC invasion, and in endometriosis invade with ESCs.

SUPPLEMENTAL FIGURES:

Figure 1 – figure supplement 1:
Immunocytochemical assessment of Epithelial and Stromal cell isolations from patients.
Cell separations from an endometriosis and control patient taken at 40x (top) and 10x (bottom), indicate the purity of the isolations, using double staining with EpCAM or cytokeratin 7 antibodies for Epithelial cells (red), and Vimentin for stromal cells (green). Nuclei are stained blue with DAPI in both. Bars are 20 µm (top) and 100 µm (bottom)

Figure 1 – figure supplement 2:
Relative invasiveness of ESCs and EECs. (accompanies **Fig. 1F**)
(A-C) ESCs [labeled with DiI (red)] and EECs [labelled with DiO (green)] were mixed in equal numbers prior to invasion across a PMC monolayer. Invading cells were visualized with DAPI (blue) to stain the nuclei. As DiI and DiO are lipophilic dyes, they stain in a non-uniform punctate pattern. The two cell types tended to invade in clusters. ESCs formed the majority of the invasive cells (A and C), although in some regions EECs represented 50% of the invasive species.
(D) In some experiments, rather than pre-labelling, the cells were fixed and stained with Vimentin for ESCs (green) and cytokeratin 7 for EECs (red). The more uniform labeling clearly demonstrates the predominance of ESCs in the invasive cells. Scale bars are 10 µm.

REFERENCES:

Augoulea, A., Alexandrou, A., Creatsa, M., Vrachnis, N and Lambrinoudaki, I. Pathogenesis of endometriosis: the role of genetics, inflammation and oxidative stress, Arch. Gynecology and Obstetrics, 286: 99-103 (2012). PMID: 22546953

Beahm DL, Oshima A, Gaietta GM, Hand GM, Smock AE, Zucker SN, Toloue MM, Chandrasekhar A, Nicholson BJ, Sosinsky GE. Mutation of a conserved threonine in the third transmembrane helix of alpha- and beta-connexins creates a dominant-negative closed gap junction channel. J Biol Chem. 281: 7994-8009 (2006) PMID: 16407179

Björk E, Israelsson P, Nagaev I, Nagaeva O, Lundin E, Ottander U, Mincheva-Nilsson L. Endometriotic Tissue–derived Exosomes Downregulate NKG2D-mediated Cytotoxicity and Promote Apoptosis: Mechanisms for Survival of Ectopic Endometrial Tissue in Endometriosis. J Immunol 213 : 567–576 (2024) PMID: 38984872

Bontempo A.C., Mikesell L., Patient perceptions of misdiagnosis of endometriosis: results from an online national survey, Diagnosis (Berl) 7: 97-106 (2020) PMID: 32007945

Burney RO, Talb S, Hamilton AE, Vo KC, Nyegaard M, Nezhat CR, et al. Gene expression of endometrioum reveals prgesterone resistance and candidate susceptibility genes in women with endometriosis. Endocrinology 148:3814-26 (2007) PMID 17510236

Burney R.O., Giudice L.C., Pathogenesis and pathophysiology of endometriosis, Fertil. Steril., 98: 511-519 (2012) PMID: 22819144

Butt H.J., and Jaschke M. Calculation of Thermal Noise in Atomic Force Microscopy. Nanotechnology 6: 1–7. (1995).

Go VAA, Chavez J, Robinson RD, Galang MA, Kumar RS, Nicholson BJ. Investigating the role of peritoneal mesothelial cells in endometriosis lesion formation. Fertility and Sterility 120: e318 (2024)

Chen Q, Boire A, Jin X, et al. Carcinoma-astrocyte gap junctions promote brain metastasis by cGAMP transfer Nature, 533: 493-498 (2016) PMID: 27225120

Chen JC, Hoffman JR, Arora R, Perrone LA, Gonzalez-Gomez CJ, Vo KC, Laird DJ, Irwin JC, Giudice LC. Cryopreservation and recovery of human endometrial epithelial cells with high viability, purity, and functional fidelity. Fertil Steril. 105: 501-10. (2016) PMID: 26515378

Chen CW, Chavez J, Lin LL, Wang CM, Hsu YT, Hart MJ, Ruan J, Gillette L, Burney RO, Schenken RS, Robinson RD, Gaczynska M, Osmulski P, Kirma NB and Nicholson BJ. Changes in Gap Junction Expression in the Endometrium are Early Indicators of Endometriosis and Integral to the Invasive Process. bioRxiv 10.1101/2021.01.25.428135v1

Cheng Y., Ma, D. Zhang Y., Li Z., Geng L. Cervical squamous cancer mRNA profiles reveal the key genes of metastasis and invasion, Eur J Gynaecol Oncol, 36: 309-317 (2015) PMID: 26189259

de Boer TP, van Veen TA, Bierhuizen MF, Kok B, Rook MB, Boonen KJ, Vos MA, Doevendans PA, de Bakker JM, van der Heyden MA. Connexin43 repression following epithelium-to-mesenchyme transition in embryonal carcinoma cells requires Snail1 transcription factor. Differentiation. 75:208-18. (2007) PMID: 17359298.

De La Garza EM, Binkley PA, Ganapathy M, Krishnegowda NK, Tekmal RR, Schenken RS, Kirma NB. Raf-1, a potential therapeutic target, mediates early steps in endometriosis lesion

development by endometrial epithelial and stromal cells. Endocrinology. 153: 3911-21. (2012) PMID: 22619359

Diao H., Xiao S., Howerth E.W, Zhao F., Li R., Ard M.B., Ye X. Broad gap junction blocker carbenoxolone disrupts uterine preparation for embryo implantation in mice, Biol. Reproduction, 89: 31. (2013) PMID: 23843229

Dufrêne YF, Ando T, Garcia R, Alsteens D, Martinez-Martin D, Engel A, Gerber C, and Müller DJ. Imaging Modes of Atomic Force Microscopy for Application in Molecular and Cell Biology. Nature Nanotechnology 12: 295–307 (2017). PMID: 28383040

el-Sabban M.E., Pauli B.U. Cytoplasmic dye transfer between metastatic tumor cells and vascular endothelium, J Cell Biology, 115: 1375-1382 (1991) PMID: 1955478

el-Sabban M.E., Pauli B.U. Adhesion-mediated gap junctional communication between lung-metastatatic cancer cells and endothelium, Invasion & Metastasis 14: 164-176 (1994) PMID: 7657509

Evans W.H., Leybaert L. Mimetic peptides as blockers of connexin channel-facilitated intercellular communication, Cell Communication & Adhesion, 14 265-273. (2007) PMID: 18392994

Eskenazi B, Warner ML. Epidemiology of endometriosis. Obstet Gynecol Clin North Am. 24:235-58 (1997) PMID: 9163765

Ferreira MC, Witz CA, Hammes LS, Kirma N, Petraglia F, Schenken RS, Reis FM. Activin A increases invasiveness of endometrial cells in an in vitro model of human peritoneum. Mol Hum Reprod. 14:301-7 (2008) PMID: 18359784

Francis R, Xu X, Park H, Wei CJ, Chang S, Chatterjee B, Lo C. Connexin43 modulates cell polarity and directional cell migration by regulating microtubule dynamics. PLoS One. 6: e26379 (2011). PMID: 22022608.

Friedrichs J, Legate KR, Schubert ., Bharadwaj M, Werner C, Müller DJ and Benoit M.. A Practical Guide to Quantify Cell Adhesion Using Single-Cell Force Spectroscopy. Methods 60: 169–78 (2013).

Go VAA, Chavez J, Robinson RD, Galang MA, Kumar RS, Nicholson BJ. Investigating the role of peritoneal mesothelial cells in endometriosis lesion formation. Fertility and Sterility 120: e318 (2024) PMID: 39121984

Goldberg GS, Lampe PD, Nicholson BJ. Selective transfer of endogenous metabolites through gap junctions composed of different connexins. Nat Cell Biol. 1:457-9 (1999). PMID: 10559992.

Grümmer R, Chwalisz K, Mulholland J, Traub O, Winterhager E. Regulation of connexin26 and connexin43 expression in rat endometrium by ovarian steroid hormones. Biol Reprod. 51:1109-16. (1994) PMID: 7888490

Grummer R., Reuss B., Winterhager E. Expression pattern of different gap junction connexins is related to embryo implantation, Intl. J. Dev. Biol. 40: 361-367. (1996) PMID: 8735949

Guo SW, Wu Y, Strawn E, Basir Z, Wang Y, Halverson G, et al. Genomic alterations in the endometrium may be a proximate cause for endometriosis. Eur J Obstet Gynecol Reprod Biol.116:89–99. (2004) PMID 15294375

Han SJ, Jung SY, Wu SP, Hawkins SM, Park MJ, Kyo S, Qin J, Lydon JP, Tsai SY, Tsai MJ, DeMayo FJ, O'Malley BW. Estrogen Receptor β Modulates Apoptosis Complexes and the Inflammasome to Drive the Pathogenesis of Endometriosis. Cell. 163:960-74 (2015). PMID: 26544941

Hastings J.M., Fazleabas A.T., A baboon model for endometriosis: implications for fertility, Reprod Biol Endocrinol, 4 (Suppl 1): S7 (2006). PMID: 17118171

Hernandez VH, Bortolozzi M, Pertegato V, Beltramello M, Giarin M, Zaccolo M, Pantano S, Mammano F. Unitary permeability of gap junction channels to second messengers measured by FRET microscopy. Nat Methods. 4:353-8. (2007) PMID: 17351620.

Hong X., Sin W.C., Harris A.L, Naus., C.C. Gap junctions modulate glioma invasion by direct transfer of microRNA, Oncotarget, 6 :15566-15577 (2015) PMID: 25978028

Hudelist G., Fritzer N., Thomas A., Niehues C., Oppelt P., Haas D., Tammaa A., Salzer H. Diagnostic delay for endometriosis in Austria and Germany: causes and possible consequences, Hum Reprod, 27: 3412-3416 (2012). PMID: 22990516

Hugo HJ, Kokkinos MI, Blick T, Ackland ML, Thompson EW, Newgreen DF. Defining the E-cadherin repressor interactome in epithelial-mesenchymal transition: the PMC42 model as a case study. Cells Tissues Organs. 193:23-40 (2011) PMID: 21051859

Ito A., Katoh F., Kataoka T.R., Okada M., Tsubota N., Asada H., Yoshikawa K., Maeda S., Kitamura Y., Yamasaki H., Nojima H. A role for heterologous gap junctions between melanoma and endothelial cells in metastasis, J. Clin. Invest. 105: 1189-1197 (2000) PMID: 10791993

Jahn E, Classen-Linke I, Kusche M, Beier HM, Traub O, Grümmer R, Winterhager E. Expression of gap junction connexins in the human endometrium throughout the menstrual cycle. Hum Reprod. 10: 2666-70 (1995). PMID: 8567789

Kanczuga-Koda L., Sulkowski S., Lenczewski A., Koda M., Wincewicz A., Baltaziak M., Sulkowska M. Increased expression of connexins 26 and 43 in lymph node metastases of breast cancer, J. Clin. Pathol. 59: 429-433. (2006) PMID: 16567471

Kaushik T., Mishra R., Singh R.K., Bajpai S. Role of connexins in female reproductive system and endometriosis, J Gynecol Obstet Hum Reprod, 49:101705. (2020) PMID: 32018041

Kirk D, Irwin JC. Normal human endometrium in cell culture. Methods Cell Biol.21B: 51-77 (1980). PMID: 7412575

Konrad L, Dietze R, Riaz MA, Scheiner-Bobis G, Behnke J, Horné F, Hoerscher A, Reising C, Meinhold-Heerlein I. Epithelial-Mesenchymal Transition in Endometriosis-When Does It Happen? J Clin Med. 9:1915. (2020) PMID: 32570986

Lamiche C., Clarhaut J., Strale P.O., Crespin S., Pedretti N., Bernard F.X., Naus C.C., Chen V.C., Foster L.J., Defamie N., Mesnil M., Debiais F., Cronier L., The gap junction protein Cx43 is involved in the bone-targeted metastatic behaviour of human prostate cancer cells. Clin. Exp. Metastasis, 29: 111-122. (2012) PMID: 22080401

Laws M.J., Taylor R.N., Sidell N., DeMayo F.J., Lydon J.P., Gutstein D.E., Bagchi M.K., Bagchi I.C. Gap junction communication between uterine stromal cells plays a critical role in pregnancy-associated neovascularization and embryo survival, Development 135: 2659-2668 (2008) PMID: 18599509

Lauchlan, S.C. The secondary Müllerian system. Obstet. Gynecol. Surv. 27, 133-146 (1972) PMID: 4614139

Lin LL, Kost ER, Lin CL, Valente P, Wang CM, Kolonin MG, Daquinag AC, Tan X, Lucio N, Hung CN, Wang CP, Kirma NB, Huang TH. PAI-1-Dependent Inactivation of SMAD4-Modulated Junction and Adhesion Complex in Obese Endometrial Cancer. Cell Rep. 33:108253 (2020). PMID: 33053339.

Lin LL, Makwana S, Chen M, Wang CM, Gillette LH, Huang TH, Burney RO, Nicholson BJ, Kirma NB. Cellular junction and mesenchymal factors delineate an endometriosis-specific response of endometrial stromal cells to the mesothelium. Mol Cell Endocrinol.539:11148 (2021). PMID: 34624439.

Lucidi RS, Witz CA, Chrisco M, Binkley PA, Shain SA, Schenken RS. A novel in vitro model of the early endometriotic lesion demonstrates that attachment of endometrial cells to mesothelial cells is dependent on the source of endometrial cells. Fertil Steril. 84:16–21 (2005) PMID: 16009148

Mettler L., Schollmeyer T., Lehmann-Willenbrock E., Schuppler U., Schmutzler A., Shukla D., Zavala A., Lewin A. Accuracy of laparoscopic diagnosis of endometriosis, JSLS, 7: 15-18 (2003). PMID: 12722993

Missmer SA, Hankinson SE, Spiegelman D, Barbieri RL, Michels KB, Hunter DJ. In utero exposures and the incidence of endometriosis. Fertil Steril. 2004; 82:1501–8. PMID: 15589850

Montgomery J, Ghatnekar GS, Grek CL, Moyer KE, Gourdie RG. Connexin 43-Based Therapeutics for Dermal Wound Healing. Int J Mol Sci. 19:1778. (2018) PMID: 29914066;

Mugisho O.O., Green C.R., Kho D.T., Zhang J., Graham E.S., Acosta M.L., Rupenthal I.D. The inflammasome pathway is amplified and perpetuated in an autocrine manner through connexin43 hemichannel mediated ATP release, Biochim Biophys Acta 1862: 385-393 (2018) PMID: 29158134

Nair AS, Nair HB, Lucidi RS, Kirchner AJ, Schenken RS, Tekmal RR *et al.* Modeling the early endometriotic lesion: mesothelium-endometrial cell co-culture increases endometrial invasion and alters mesothelial and endometrial gene transcription. Fertil. and Steril. 90:1487-95 (2008). PMID: 18163995

Nair R.R., Jain M., Singh K. Reduced expression of gap junction gene connexin 43 in recurrent early pregnancy loss patients, Placenta 32: 619-621 (2011) PMID: 21669459

Naoi Y., Miyoshi Y., Taguchi T., Kim S.J., Arai T., Tamaki Y., Noguchi S. Connexin26 expression is associated with lymphatic vessel invasion and poor prognosis in human breast cancer, Breast Cancer Res.Treat. 106: 11-17 (2007) PMID: 17203385

Nirgianakis K, Ma L, McKinnon B, Mueller MD. Recurrence Patterns after Surgery in Patients with Different Endometriosis Subtypes: A Long-Term Hospital-Based Cohort Study. J Clin Med. 9: 496-597. (2020). PMID: 32054117

Oosterlynck DJ, Cornillie FJ, Waer M, Vandeputte M, Koninckx PR. Women with endometriosis show a defect in natural killer activity resulting in a decreased cytotoxicity to autologous endometrium. Fertil Steril. 56:45–51 (1991) PMID: 2065804

Ormonde S, Chou CY, Goold L, Petsoglou C, Al-Taie R, Sherwin T, McGhee CN, Green CR. Regulation of connexin43 gap junction protein triggers vascular recovery and healing in human ocular persistent epithelial defect wounds. J Membr Biol. 245:381-8. (2012) PMID: 22797940.

945 Ornatsky O, Bandura D, Baranow V. Nitz M, Winnik MA, Tanner S. Highly multiparametric
946 analysis by mass cytometry. J. Immunological Methods. 361:1-20 (2010).

947 Parente Barbosa C., Bentes De Souza A. M., Bianco B., and Christofolini D. M. The effect of
948 hormones on endometriosis development, Minerva Ginecol. 63: 375–386 (2011).
949 PMID: 21747346

950 Polusani SR, Huang YW, Huang G, Chen CW, Wang CM, Lin LL, Osmulski P, Lucio ND, Liu L,
951 Hsu YT, Zhou Y, Lin CL, Aguilera-Barrantes I, Valente PT, Kost ER, Chen CL, Shim EY, Lee
952 SE, Ruan J, Gaczynska ME, Yan P, Goodfellow PJ, Mutch DG, Jin VX, Nicholson BJ, Huang
953 TH, Kirma NB. Adipokines Deregulate Cellular Communication via Epigenetic Repression
954 of *Gap Junction* Loci in Obese Endometrial Cancer. Cancer Res. 79:196-208 (2019) PMID:
955 30389702

956 Regidor P.A., Regidor M., Schindler A.E., Winterhager E. Aberrant expression pattern of gap
957 junction connexins in endometriotic tissues, Mol. Human Reprod. 3: 375-381 (1997)
958 PMID: 9239721

959 Reymond N, d'Água BB, Ridley AJ. Crossing the endothelial barrier during metastasis. Nat
960 Rev Cancer. 13: 858-70. (2013) PMID: 24263189

961 Richard S, Baltz JM. Prophase I arrest of mouse oocytes mediated by natriuretic peptide
962 precursor C requires GJA1 (connexin-43) and GJA4 (connexin-37) gap junctions in the antral
963 follicle and cumulusoocyte complex. Biol. Reprod. 90:137 (2014). PMID: 24804968

964 Roca-Cusachs P, Conte V, and Trepat X. Quantifying Forces in Cell Biology. Nature Cell
965 Biology 19: 742–51 (2017). PMID 28628082

966 Rogers P.A., D'HoogheT.M., Fazleabas A., Gargett C.E., Giudice L.C., Montgomery G.W.,
967 Rombauts L., Salamonsen L.A., Zondervan K.T., Priorities for endometriosis research:
968 recommendations from an international consensus workshop, Reprod Sci, 16: 335-346 (2009)
969 PMID: 19196878

970 Ruan J, Zhang W. Identifying network communities with a high resolution. Phys Rev E Stat
971 Nonlin Soft Matter Phys. 77: 016104 (2008). PMID: 18351912.

972 Ruan J. A Fully Automated Method for Discovering Community Structures in High Dimensional
973 Data. Proc IEEE Int Conf Data Min. 968-973. (2009). PMID: 25296858

974 Sampson J.A. Peritoneal endometriosis due to menstrual dissemination of endometrial tissue
975 into the peritoneal cavity. Am J Obstet Gynecol. 14: 422-469 (1927)

976 Sasson IE, Taylor HS. Stem cells and the pathogenesis of endometriosis. Ann N Y Acad Sci.
977 1127:106–15. (2008) PMID: 18443337

978 Sancho A., Vandersmissen I, Craps S, Luttun A, and Groll J. A New Strategy to Measure
979 Intercellular Adhesion Forces in Mature Cell-Cell Contacts. Scientific Reports 7: 46152 (2017).
980 PMID 28393890

981 Shafrir AL, Farland LV, Shah DK, Harris HR, Kvaskoff M, Zondervan K, Missmer SA. Risk for
982 and consequences of endometriosis: a critical epidemiologic review. Best Pract Res Clin
983 Obstet Gynaecol 51:1-15 (2018). PMID: 30017581

984 Simon AM, Goodenough DA, Li E, Paul DL. Female infertility in mice lacking connexin
985 37. Nature 385:525–29 (1997) PMID: 9020357

Singh D, Solan JL, Taffet SM, Javier R, Lampe PD. Connexin 43 interacts with zona occludens-1 and -2 proteins in a cell cycle stage-specific manner. J Biol Chem. 280:30416-21. (2005) PMID: 1598042..

Sneddon IN. “The Relation between Load and Penetration in the Axisymmetric Boussinesq Problem for a Punch of Arbitrary Profile.” International Journal of Engineering Science 3: 47–57 (1965).

Sokolov, I, and Dokukin M. Mechanics of Biological Cells Studied with Atomic Force Microscopy. Microscopy and Microanalysis 20: 2076–77 (2014).

Soliman A.M., Yang H., Du E.X., Kelley C., Winkel C. The direct and indirect costs associated with endometriosis: a systematic literature review, Hum Reprod, 31: 712-722 (2016) PMID: 26851604

Somigliana E, Vigano P, Gaffuri B, Guarneri D, Busacca M, Vignali M. Human endometrialnstromal cells as a source of soluble intercellular adhesion molecule (ICAM)-1 molecules. HumnReprod. 11:1190–4 (1996) PMID 8671421

Stoletov K., Strnadel J., Zardouzian E., Momiyama M., Park F.D., Kelber J.A., Pizzo D.P., Hoffman R., VandenBerg S.R., Klemke R.L. Role of connexins in metastatic breast cancer and melanoma brain colonization, J Cell Sci. 126: 904-913. (2013) PMID: 23321642

Tamaresis J.S., Irwin J.C., Goldfien G.A., Rabban J.T., Burney R.O., Nezhat C., DePaolo L.V., Giudice L.C., Molecular classification of endometriosis and disease stage using high-dimensional genomic data, Endocrinology, 155: 4986-4999 (2014) PMID: 25243856

Taniguchi F, Kaponis A, Izawa M, Kiyama T, Deura I, Ito M, Iwabe T, Adonakis G, Terakawa N, Harada T. Apoptosis and endometriosis. Front Biosci 3 :648-62. (2011). PMID: 21196342.

Taubenberger AV., Hutmacher DW, and Muller DJ. Single-Cell Force Spectroscopy, an Emerging Tool to Quantify Cell Adhesion to Biomaterials. Tissue Engineering Part B: Reviews 20: 40–55 (2014)

Ulukus M., Cakmak H., Arici A. The role of endometrium in endometriosis, J Soc Gynecol Investig, 13: 467-476 (2006) PMID: 16990031

Wu JI, Wang LH. Emerging roles of gap junction proteins connexins in cancer metastasis, chemoresistance and clinical application. J Biomed Sci. 26:8-22 (2019) PMID: 30642339

Weber PA, Chang HC, Spaeth KE, Nitsche JM, Nicholson BJ. The permeability of gap junction channels to probes of different size is dependent on connexin composition and permeant-pore affinities. Biophys J. 87:958-73. (2004) PMID: 15298902.

Willebrords J, Crespo Yanguas S, Maes M, Decrock E, Wang N, Leybaert L, Kwak BR, Green CR, Cogliati B, Vinken M. Connexins and their channels in inflammation. Crit Rev Biochem Mol Biol. 51:413-439 (2016). PMID: 27387655

Winterhager E, Grümmer R, Mavrogianis PA, Jones CJ, Hastings JM, Fazleabas AT. Connexin expression pattern in the endometrium of baboons is influenced by hormonal changes and the presence of endometriotic lesions. Mol Hum Reprod. 15:645-52. (2009) PMID: 19661121

Winterhager E., Kidder G.M. Gap junction connexins in female reproductive organs: implications for women's reproductive health, Hum Reprod Update, 21: 340-352. (2015) PMID: 25667189

Yu J., Boicea A., Barrett K.L., James C.O., Bagchi I.C., Bagchi M.K, Nezhat C., Sidell N., Taylor R.N., Reduced connexin 43 in eutopic endometrium and cultured endometrial stromal cells from subjects with endometriosis, Mol. Human Reprod. 20: 260-270 (2014) PMID: 24270393

Zhang A., Hitomi M., Bar-Shain N., Dalimov Z., Ellis L., Velpula K.K., Fraizer G.C., Gourdie R.G., Lathia J.D. Connexin 43 expression is associated with increased malignancy in prostate cancer cell lines and functions to promote migration, Oncotarget, 6: 11640-11651 (2015) PMID: 25960544

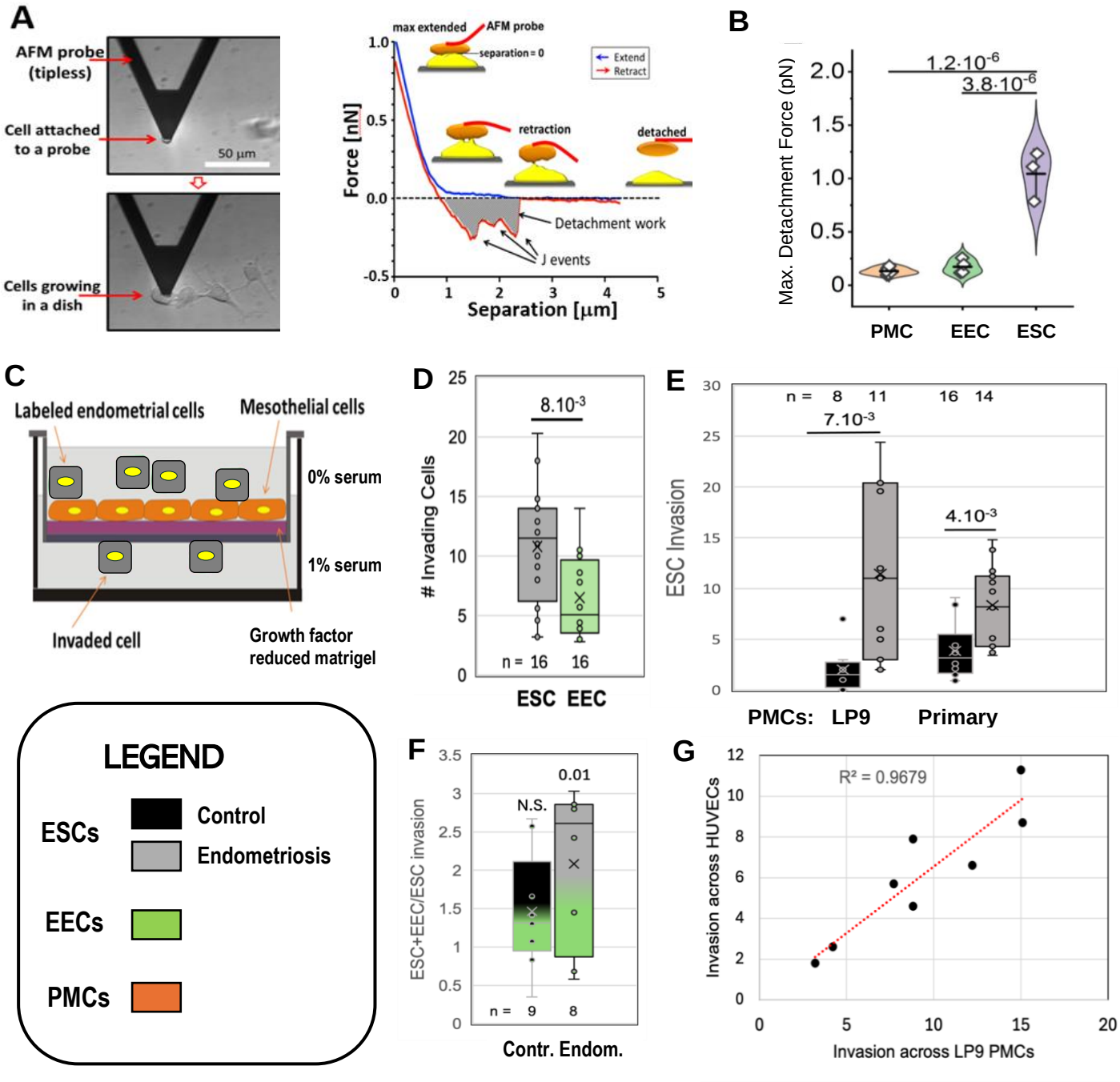
A
AFM probe (tipless)
Cell attached to a probe
50 µm
Cells growing in a dish
max extended
AFM probe
separation = 0
Extend
Retract
retraction
detached
Detachment work
J events
Force [nN]
Separation [µm]
B
Max. Detachment Force (pN)
1.2·10-6
3.8·10-6
PMC
EEC
ESC
C
Labeled endometrial cells
Mesothelial cells
0% serum
1% serum
Invaded cell
Growth factor reduced matrigel
D
Invading Cells
8.10-3
n = 16 16
ESC EEC
E
ESC Invasion
n = 8 11 16 14
7.10-3
4.10-3
PMCs: LP9 Primary
LEGEND
ESCs
Control
Endometriosis
EECs
PMCs
F
ESC+EEC/ESC invasion
0.01
N.S.
n = 9 8
Contr. Endom.
G
R² = 0.9679
Invasion across HUVECs
Invasion across LP9 PMCs

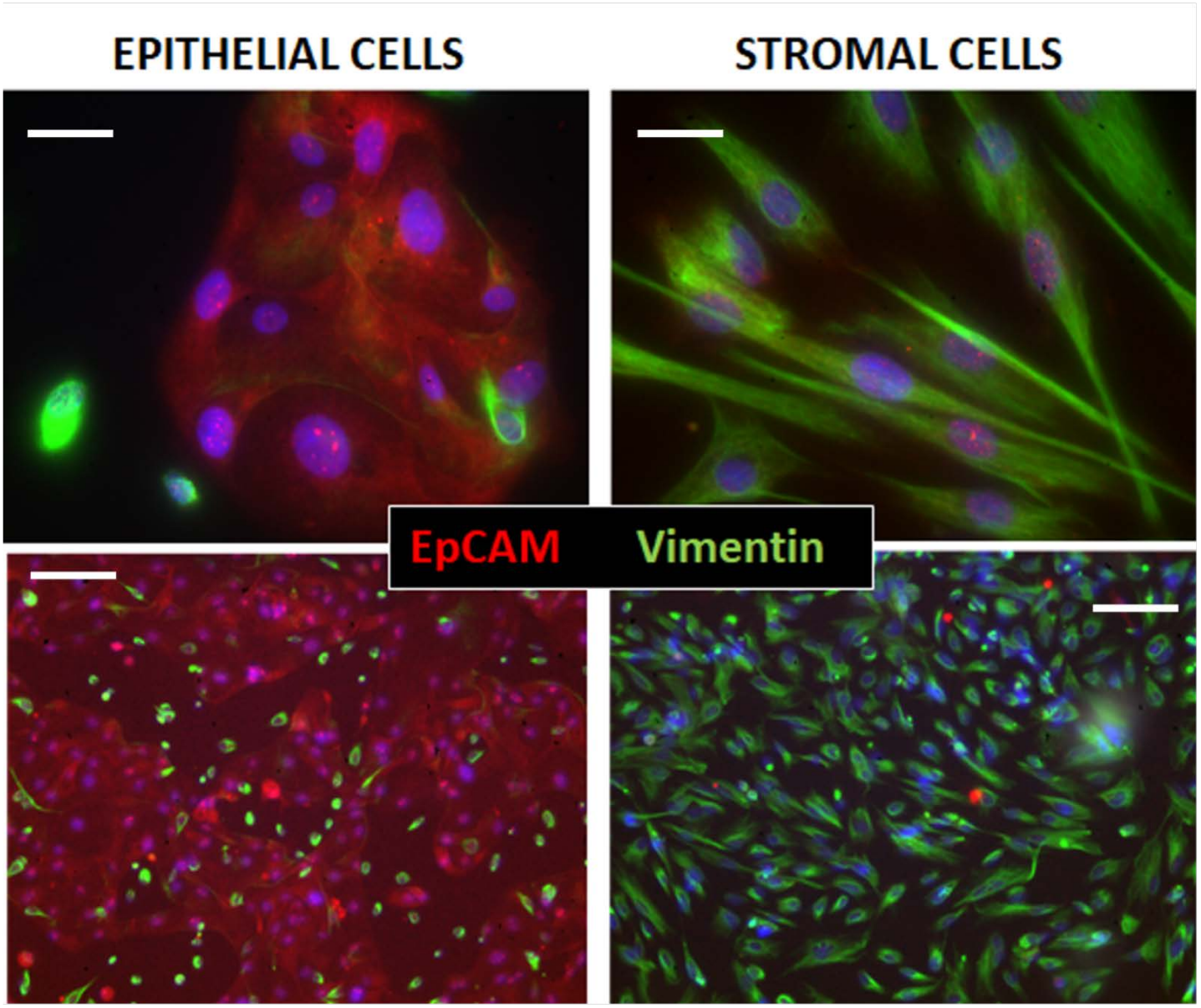

Fig. S1: Immunocytochemical assessment of Epithelial and Stromal cell isolations from patients.

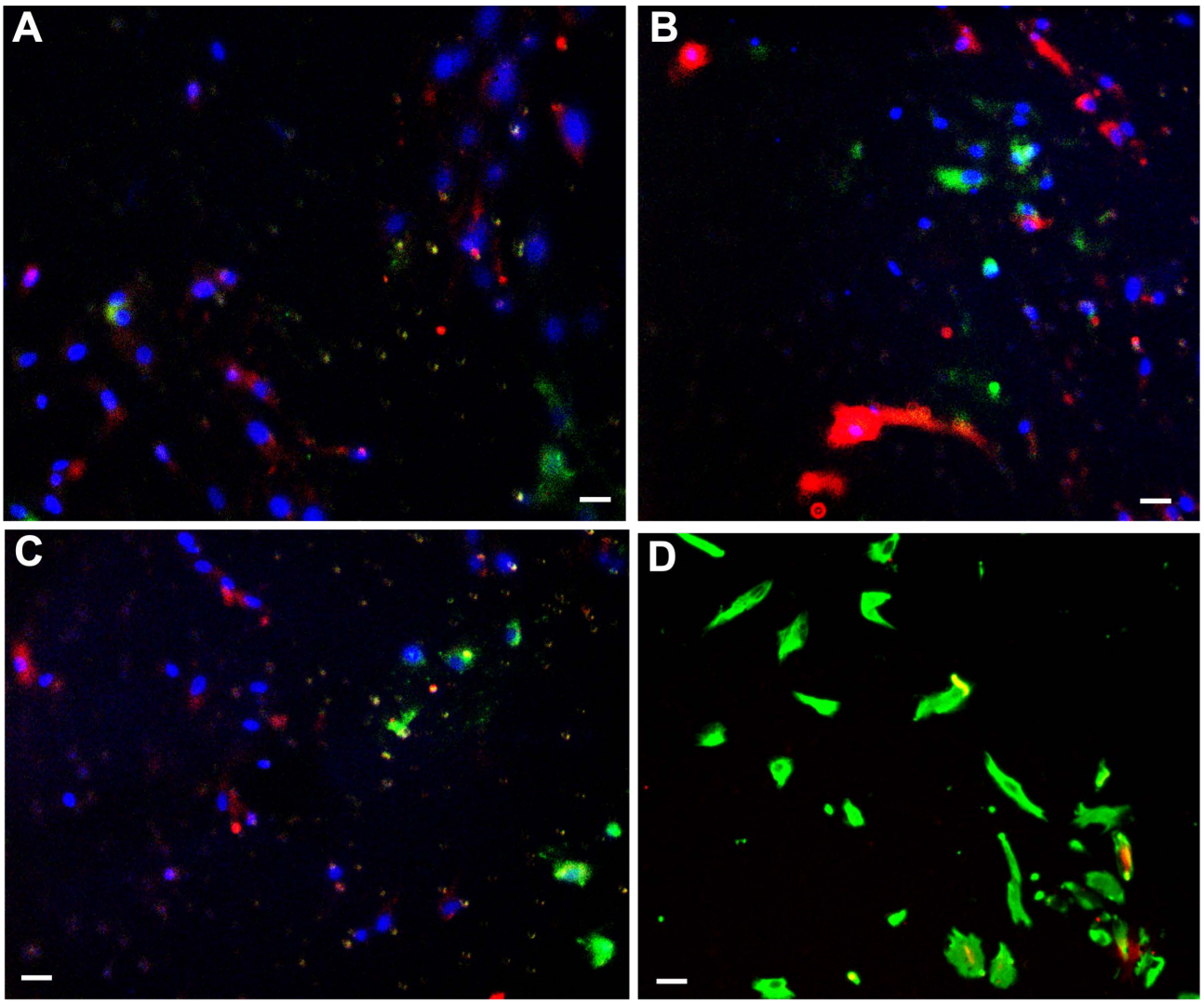

Fig. S2: **Relative invasiveness of ESCs and EECs.** **(accompanies Fig. 1E)**

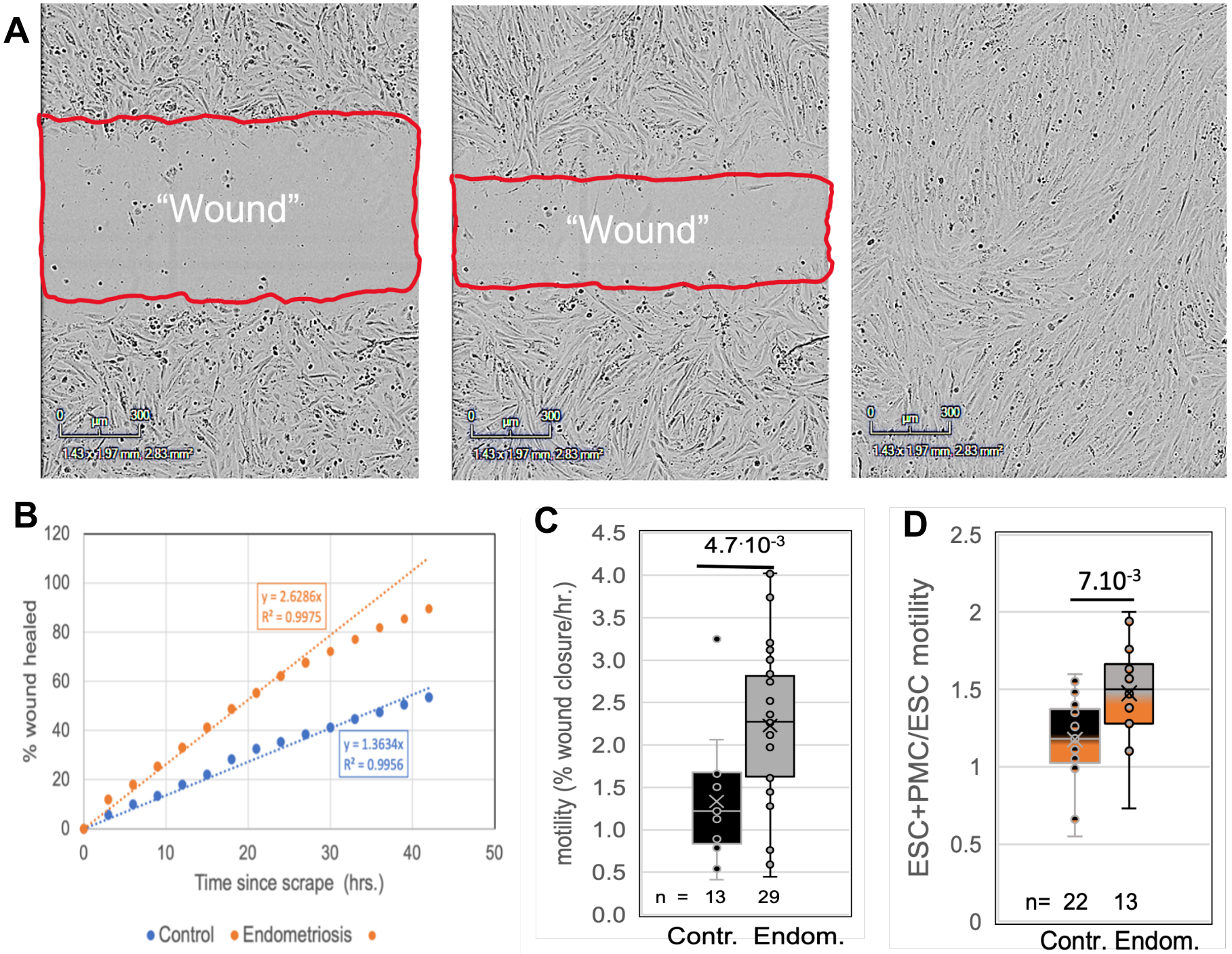
A
"Wound"
"Wound"
0 µm 300
1.43 x 1.97 mm, 2.83 mm²
B
% wound healed
y = 2.6286x
R² = 0.9975
y = 1.3634x
R² = 0.9956
Time since scrape (hrs.)
Control
Endometriosis
C
motility (% wound closure/hr.)
4.7·10-3
n = 13 29
Contr. Endom.
D
ESC+PMC/ESC motility
7.10-3
n= 22 13
Contr. Endom.

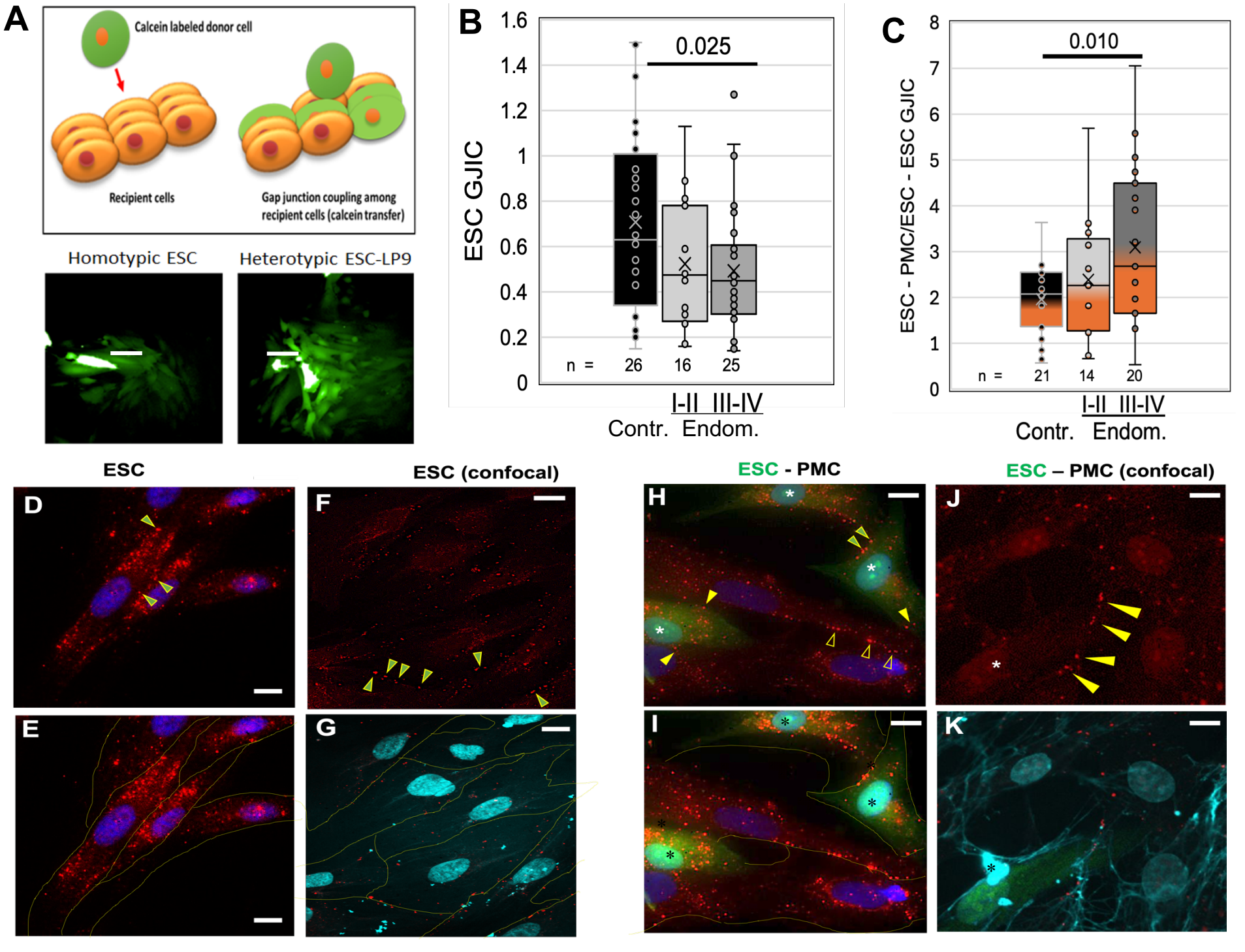
A
Calcein labeled donor cell
Recipient cells
Gap junction coupling among recipient cells (calcein transfer)
Homotypic ESC
Heterotypic ESC-LP9
B
ESC GJIC
1.6
1.4
1.2
1
0.8
0.6
0.4
0.2
0
0.025
n = 26 16 25
I-II III-IV
Contr. Endom.
C
ESC - PMC/ESC - ESC GJIC
8
7
6
5
4
3
2
1
0
0.010
n = 21 14 20
I-II III-IV
Contr. Endom.
ESC
ESC (confocal)
ESC - PMC
ESC – PMC (confocal)
D
E
F
G
H
I
J
K

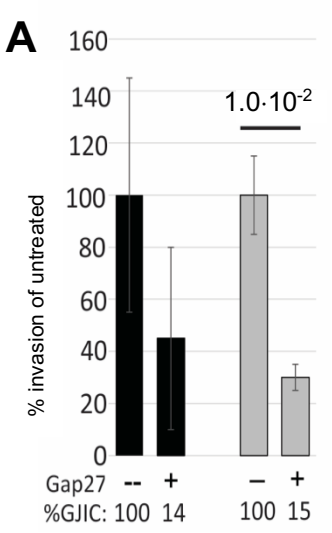
A
160
140
120
100
80
60
40
20
0
% invasion of untreated
1.0·10-2
Gap27 -- + – +
%GJIC: 100 14 100 15

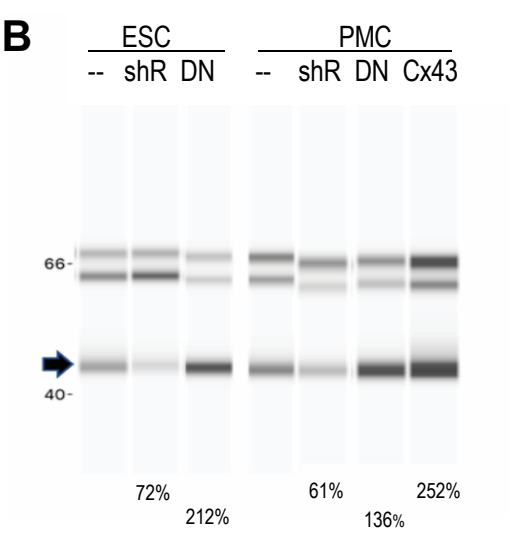
B
ESC
PMC
-- shR DN -- shR DN Cx43
66-
40-
72%
212%
61%
252%
136%

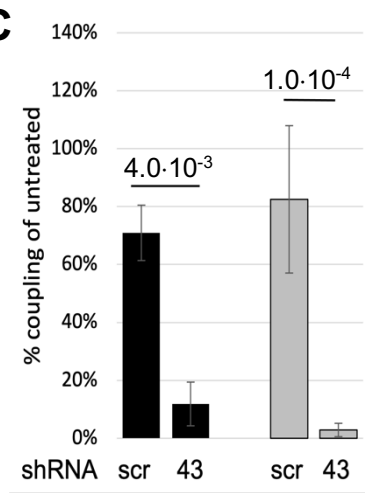
C
140%
120%
100%
80%
60%
40%
20%
0%
% coupling of untreated
4.0·10-3
1.0·10-4
shRNA scr 43 scr 43

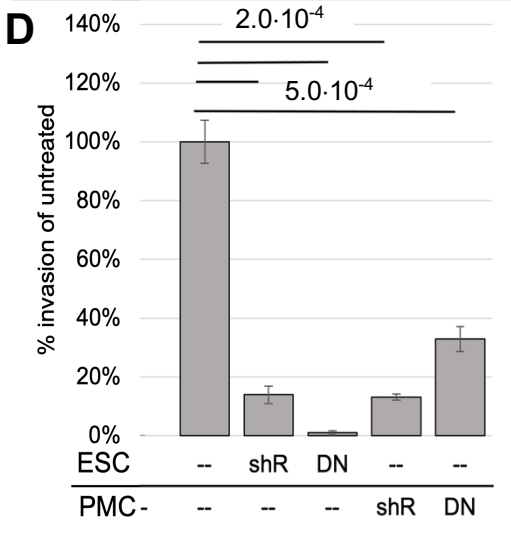
D
140%
120%
100%
80%
60%
40%
20%
0%
% invasion of untreated
2.0·10-4
5.0·10-4
ESC -- shR DN -- --
PMC - -- -- -- shR DN

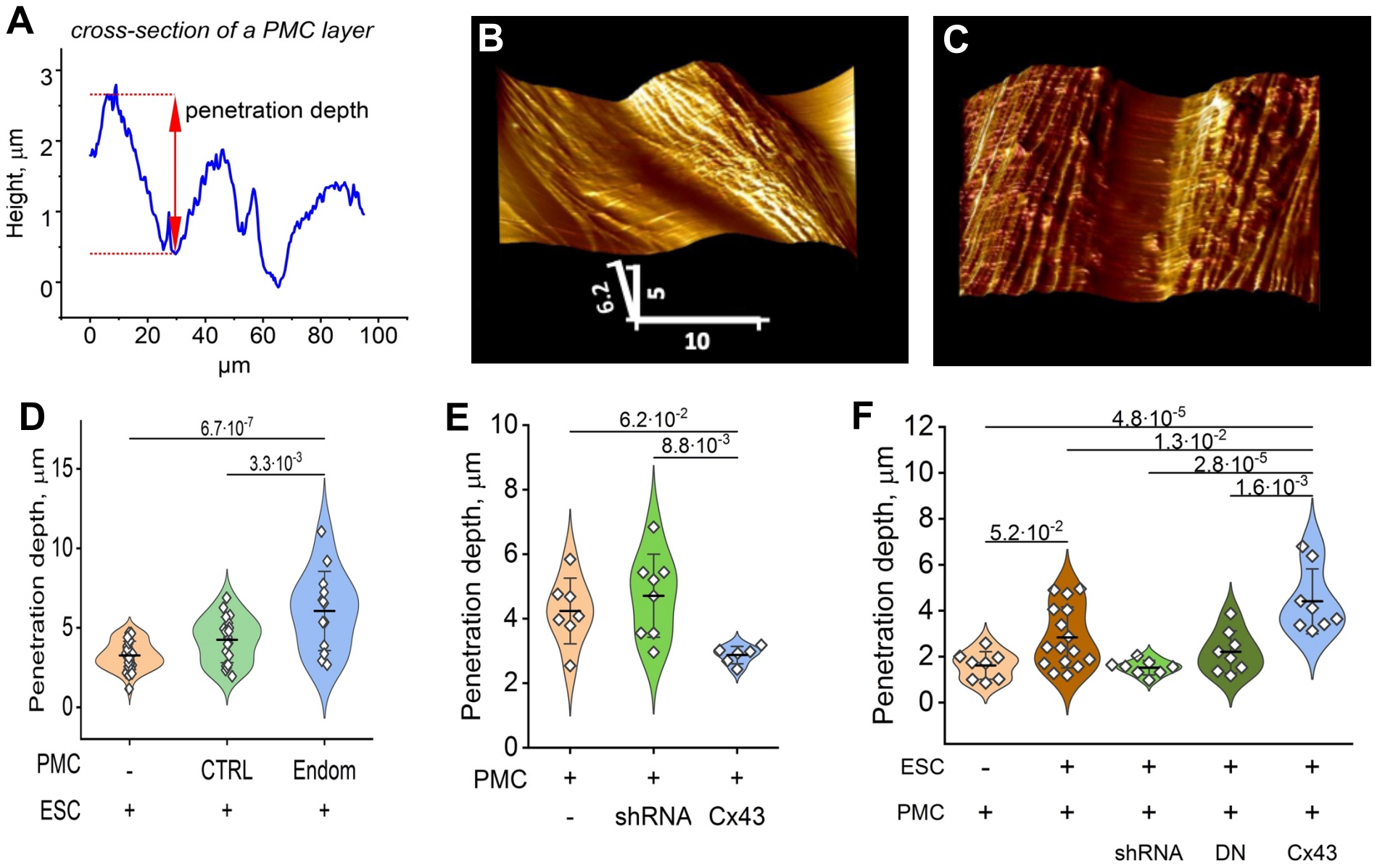
A
cross-section of a PMC layer
penetration depth
Height, µm
µm
B
C
6.2
5
10
D
6.7·10-7
3.3·10-3
Penetration depth, µm
PMC - CTRL Endom
ESC + + +
E
6.2·10-2
8.8·10-3
Penetration depth, µm
PMC + + +
- shRNA Cx43
F
4.8·10-5
1.3·10-2
2.8·10-5
1.6·10-3
5.2·10-2
Penetration depth, µm
ESC - + + + +
PMC + + + + +
shRNA DN Cx43

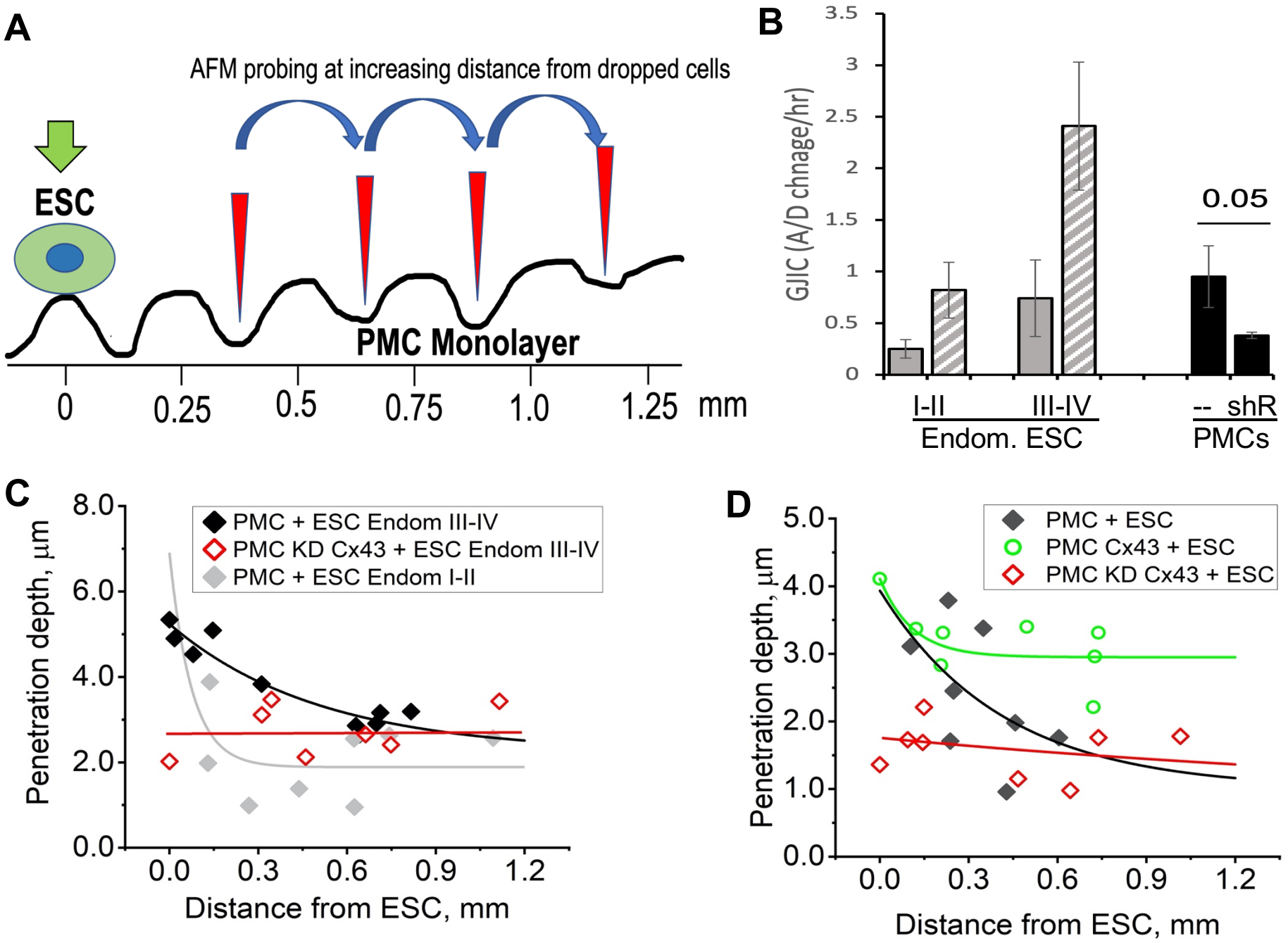
A
AFM probing at increasing distance from dropped cells
ESC
PMC Monolayer
0
0.25
0.5
0.75
1.0
1.25
mm
B
GJIC (A/D chnage/hr)
3.5
3
2.5
2
1.5
1
0.5
0
0.05
I-II
III-IV
Endom. ESC
-- shR
PMCs
C
Penetration depth, µm
8.0
6.0
4.0
2.0
0.0
PMC + ESC Endom III-IV
PMC KD Cx43 + ESC Endom III-IV
PMC + ESC Endom I-II
0.0
0.3
0.6
0.9
1.2
Distance from ESC, mm
D
Penetration depth, µm
5.0
4.0
3.0
2.0
1.0
0.0
PMC + ESC
PMC Cx43 + ESC
PMC KD Cx43 + ESC
0.0
0.3
0.6
0.9
1.2
Distance from ESC, mm

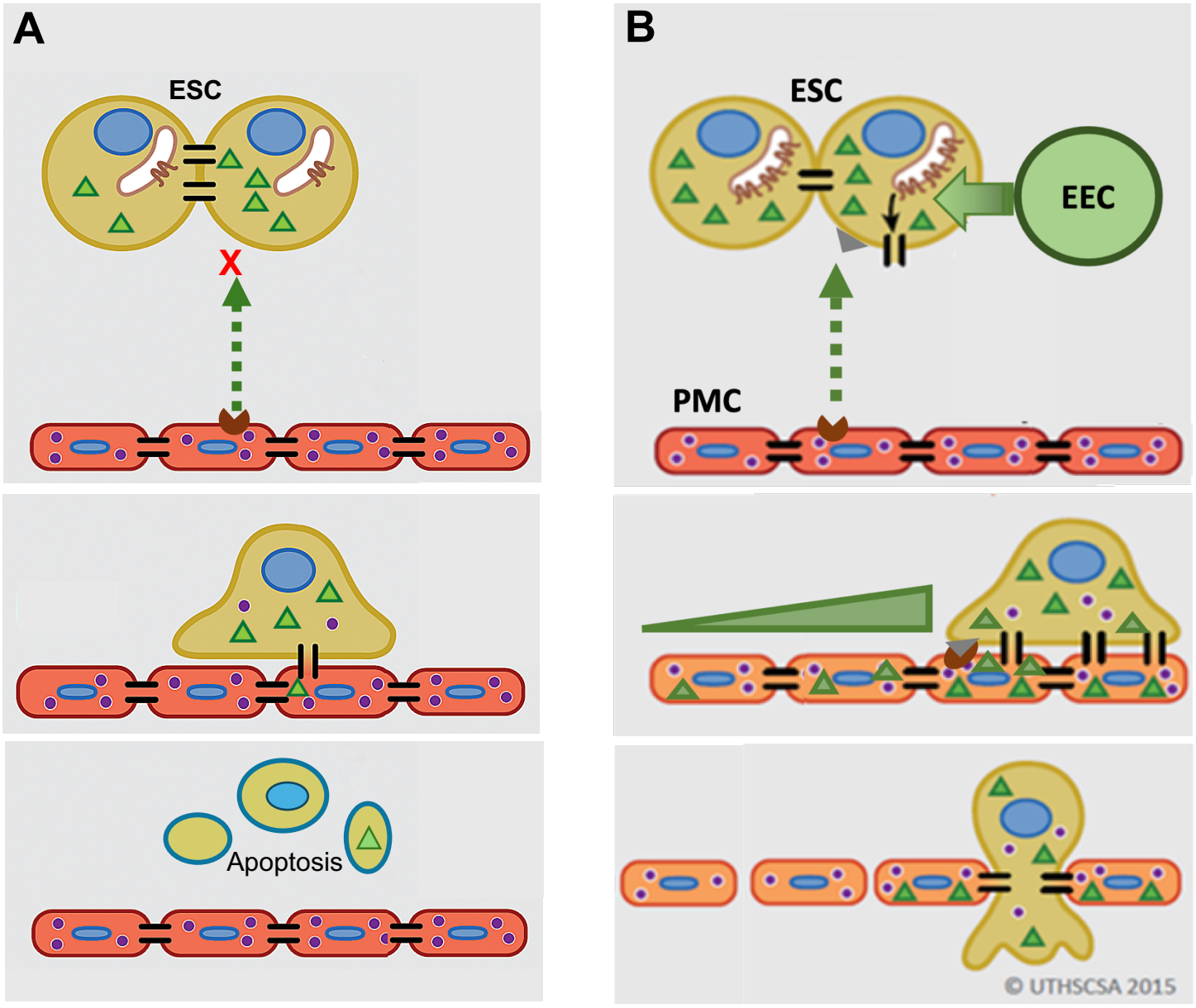
A
ESC
X
B
ESC
EEC
PMC
Apoptosis
© UTHSCSA 2015